[American Journal of Science, Vol. 305, January, 2005, P. 1–41]

American Journal of Science

JANUARY 2005

DATING PLIO-PLEISTOCENE GLACIAL SEDIMENTS USING THE COSMIC-RAY-PRODUCED RADIONUCLIDES ^{10}Be AND ^{26}Al

GREG BALCO*,†, JOHN O.H. STONE*, and CARRIE JENNINGS**

ABSTRACT. We use the cosmic-ray-produced radionuclides ^{26}Al and ^{10}Be to date Plio-Pleistocene glacial sediment sequences. These two nuclides are produced in quartz at a fixed ratio, but have different decay constants. If a sample is exposed at the surface for a time and then buried by overburden and thus removed from the cosmic-ray flux, the ^{26}Al/^{10}Be ratio is related to the duration of burial. We first attempted to date pre-Wisconsinan tills by measuring ^{26}Al and ^{10}Be in fluvial sediments beneath them and applying the method of "burial dating," which previous authors have used to date river sediment carried into caves. This method, however, requires simplifying assumptions about the ^{26}Al and ^{10}Be concentrations in the sediment at the time of burial. We show that these assumptions are not valid for river sediment in glaciated regions. ^{26}Al and ^{10}Be analyses of such sediment do not provide accurate ages for these tills, although they do yield limiting ages in some cases. We overcome this difficulty by instead measuring ^{26}Al and ^{10}Be in quartz from paleosols that are buried by tills. We use a more general mathematical approach to determine the initial nuclide concentrations in the paleosol at the time it was buried, as well as the duration of burial. This technique provides a widely applicable improvement on other means of dating Plio-Pleistocene terrestrial glacial sediments, as well as a framework for applying cosmogenic-nuclide dating techniques in complicated stratigraphic settings. We apply it to pre-Wisconsinan glacial sediment sequences in southwest Minnesota and eastern South Dakota. Pre-Wisconsinan tills underlying the Minnesota River Valley were deposited 0.5 to 1.5 Ma, and tills beneath the Prairie Coteau in eastern South Dakota and adjacent Minnesota were deposited 1 to 2 Ma.

INTRODUCTION: PURPOSE OF THIS STUDY

In this paper we describe our efforts to better determine the timing of Plio-Pleistocene ice sheet advances by using the cosmic-ray-produced nuclides ^{10}Be and ^{26}Al to date glacial sediments.

The chief motivation for this work is the need for new methods to determine the age of the thick sequences of tills and associated ice-marginal sediments that surround the locations of former continental ice sheets in North America and Eurasia. These deposits are important because they record the advances and retreats of the large ice sheets that are the defining feature of the last several million years of Earth history. Despite this direct stratigraphic evidence of many glaciations, however, most information about the timing of ice sheet advances prior to the most recent Wisconsinan glaciation comes from oxygen-isotope records in marine sediment cores that are dated by paleomagnetic stratigraphy and astronomical tuning (Emiliani, 1955; Shackleton and Opdyke, 1973). These δ^{18}O time-series record only global ice volume. Except in rare cases where ice-rafted debris in sediment cores can be associated with a specific

*Quaternary Research Center and Department of Earth and Space Sciences, University of Washington, Mail Stop 351310, Seattle, Washington 98195-1310 USA
**Minnesota Geological Survey, 2642 University Avenue W., St. Paul, Minnesota 55114-1057 USA
†Corresponding author: balcs@u.washington.edu

source (for example, Shackleton and others, 1984; Mangerud and others, 1996; Hambrey and others, 2002), marine records give little information about the location of ice on the continents or the partitioning of ice between different ice sheets. The continental deposits that would provide this information are extremely difficult to date. In the region formerly occupied by the Laurentide Ice Sheet, for example, the only means available for dating sediments older than the useful ranges of radiocarbon (~50,000 yr) or optical dating techniques (~150,000 yr) are by bracketing them between two easily recognized magnetic reversals [0.78, 2.58 Ma; Cande and Kent (1995)] or three widespread ashes from the Yellowstone volcanic center [0.6, 1.3, and 2.0 Ma; Gansecki and others (1998)]. As only a few sections contain any of these time markers at all, it is impossible to associate most individual pre-Wisconsinan tills with particular marine oxygen isotope stages, and there exists little direct evidence to show whether or not the configuration of ice sheets during most older glaciations was or was not similar to that during the most recent one.

Besides this particular question of the age of Plio-Pleistocene glacial sediments, we are interested in expanding the range of applications of cosmogenic-nuclide geochronology. To date, measurements of cosmic-ray-produced radionuclides have been used almost exclusively for exposure-age dating of surface rocks (Gosse and Phillips, 2001). Only a few authors have attempted to use more complicated methods that rely on the decay of these nuclides as well as their initial accumulation (for example, Granger and Muzikar, 2001; Wolkowinsky and Granger, 2004). Here we describe methods for using the two radionuclides ^{10}Be and ^{26}Al to date stratified deposits in complex geologic settings. These nuclides have half-lives that are suited to dating sediments deposited 0.5 to 3 Ma, and occur in quartz, which is ubiquitous in sedimentary systems. Although we discuss only glacial sediments in this paper, the methods we describe apply to Plio-Pleistocene clastic sediments in general, and could be used in many sedimentary environments.

THE BASICS OF ^{26}Al AND ^{10}Be DATING METHODS

^{26}Al and ^{10}Be are rare radionuclides that accumulate in quartz subjected to cosmic ray bombardment near the Earth's surface. These nuclides are commonly used for exposure-age dating, which relies on the fact that they are produced at a known rate in rock surfaces exposed to the surface cosmic ray flux (for example, Gosse and Phillips, 2001). Here we are not concerned with exposure dating of surfaces, but with another technique, sometimes known as "burial dating," which relies on the fact that ^{26}Al and ^{10}Be are produced at a fixed ratio, but have different decay constants. If sedimentary quartz exposed at the Earth's surface for enough time to develop measurable quantities of these nuclides is then buried below the surface – and thus isolated from the cosmic-ray flux – the two nuclides decay at different rates, and the ^{26}Al/^{10}Be ratio reflects the duration of burial (for example, Klein and others, 1988; Lal, 1988). In this section, we first describe the basis for previous uses of burial dating in simple geologic situations, and then describe the additional complications that arise, and the different approach that is required, when using the technique to date stratified sediments.

Depth Dependence of ^{26}Al and ^{10}Be Production

At the Earth's surface, ^{26}Al and ^{10}Be production in quartz is mostly by spallation reactions on O and Si, and to a much lesser extent by negative muon capture and fast muon interactions (Lal and Peters, 1967). The total surface production rates of these nuclides in quartz at sea level and high latitude are approximately 5.1 and 31.1 atoms g^{-1} yr^{-1} for ^{10}Be and ^{26}Al respectively (Stone, 2000). These production rates vary predictably with latitude, altitude, and magnetic field variation (Lal, 1991; Stone, 2000; Gosse and Phillips, 2001), but the ratio of ^{26}Al and ^{10}Be production rates is fixed at 6.1 (Nishiizumi and others, 1989). Some details of surface production are still the subject

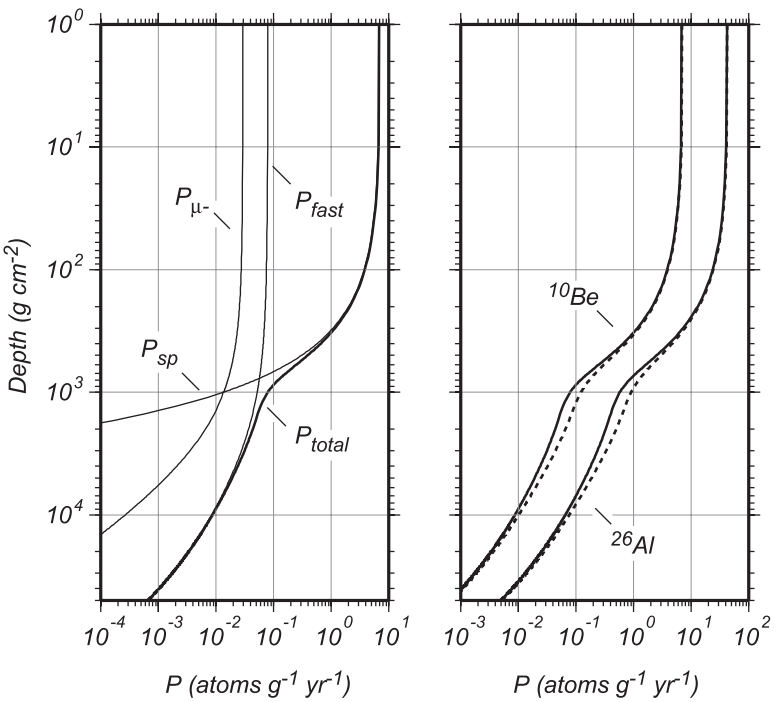

Fig. 1. Depth dependence of ^{26}Al and ^{10}Be production rates. Left panel, contribution of spallation (P_{sp}), negative muon capture ($P_{\mu-}$), and fast muon interactions (P_{fast}) to ^{10}Be production in quartz. Surface production rate of ^{10}Be by spallation assumed to be 7 atoms g^{-1} yr^{-1}. P_{fast} and $P_{\mu-}$ are calculated using muon interaction cross-sections inferred from measurements at Wyangla Quarry, Australia, as described in text (J. Stone, unpublished data). Right panel, effect of uncertainty in muon interaction cross-sections on total production rates of ^{10}Be and ^{26}Al. Solid lines, Wyangla Quarry cross-sections; dashed lines, cross-sections from Heisinger (2002a, 2002b).

of active research; these remaining uncertainties in surface production rate estimates are not significant in the context of this paper and we do not dwell on them.

Nuclide production rates decrease with depth below the ground surface (fig. 1). In order to simplify the text and mathematics in this paper, we describe depth in units of g cm^{-2} to reflect the attenuation of the cosmic-ray flux according to the amount of mass traversed. This measure of depth is sometimes referred to as "mass depth" or "shielding depth." If d is linear depth below the surface (cm) and ρ is the density of the overburden (g cm^{-3}), $z = d\rho$.

The depth dependence of the production rate of nuclide j due to spallation is:

$$P_{sp,j}(z) = P_{sp,j}(0)e^{(-z/\Lambda_{sp})} \quad (1)$$

where z is depth below the surface (g cm^{-2}), $P_{sp,j}(z)$ the production rate due to spallation at depth z (atoms g^{-1} yr^{-1}), $P_{sp,j}(0)$ the surface production rate due to spallation (atoms g^{-1} yr^{-1}), and Λ_{sp} the effective attenuation length (g cm^{-2}) for spallation. Here we use $\Lambda_{sp} = 160$ g cm^{-2} (see Gosse and Phillips, 2001, for a discussion of this choice). For depths less than approximately 500 g cm^{-2}, production by spallation dominates, and equation (1) is a good approximation for the total production rate $P_j(z)$.

Production due to muon reactions is attenuated much less rapidly than spallogenic production, and predominates at greater depths (fig. 1). Both the depth

dependence of the muon flux and the nuclear cross-sections for muon interactions are the subject of active research at present. In this work we wish to give an idea of how important the uncertainty in these parameters is to our results, without quantifying it in a way that may later prove to be wrong. The few measurements of the relevant quantities, in particular the cross-sections, are subject to systematic as well as random errors, and offer no basis for selecting a Gaussian or any other probability distribution to describe the uncertainty. Thus, we proceed as follows. We use the compilation of sea level/high latitude measurements of the subsurface muon flux from Heisinger and others (2002a). As our sites are near 45°N latitude and at 400 to 600 m elevation, we expect this to be a good approximation for the actual muon flux at depths greater than 2000 g cm^{-2}. We then perform most calculations using two sets of cross-sections for production of ^{10}Be and ^{26}Al by negative muon capture and fast muon interactions: first, those measured experimentally by Heisinger and others (2002a, 2002b), and second, those inferred from a quarry profile at Wyangla, Australia (Stone, J., unpublished data). The values measured by Heisinger and others (2002a, 2002b) are as follows: the energy dependence exponent for fast muon interactions α is 0.75 (see Heisinger and others, 2002a, eq 13), and the effective nuclide production probabilities after muon capture f^* are 0.43 percent and 2.2 percent for ^{10}Be from O in SiO_2) and ^{26}Al from Si in SiO_2), respectively (see Heisinger and others, 2002b, eq 11). The corresponding values inferred from the Wyangla quarry profile are α=0.8, f^* = 0.12 percent for ^{10}Be, and f^* =0.62 percent for ^{26}Al. The range in production rates generated by these two sets of parameters is representative of the uncertainty in our present knowledge of subsurface production rates. The resulting production rates differ by a factor of two or more at depths of 500 to 2000 g cm^{-2}, but are similar near the surface and at depths greater than 10,000 g cm^{-2} (fig. 1). Thus, the uncertainty in these parameters is most important when samples are buried at shallow depths for long periods of time, and is not important when samples are deeply buried.

^{26}Al/^{10}Be Dating of Buried Sediments in Simple Situations

Here we describe the approach used in previous studies that applied ^{26}Al and ^{10}Be measurements to date buried sediments (Klein and others, 1988; Granger and Muzikar, 2001). We are interested in samples of quartz that were exposed at the surface for a time and then buried at a known depth below the surface. First, we consider the period of exposure. If a sample begins with zero initial ^{26}Al and ^{10}Be concentrations, then is continuously exposed at the surface for an exposure time t_{exp} (yr), while eroding at a constant rate ϵ (g cm^{-2} yr^{-1}), the concentration $N_j(t_{exp})$ (atoms g^{-1}) of nuclide j is:

$$N_j(t_{exp}) = \frac{P_j(0)}{\lambda_j + \frac{\epsilon}{\Lambda_{sp}}} \left(1 - e^{-(\lambda_j + (\epsilon/\Lambda_{sp}))t_{exp}}\right) \quad (2)$$

where $P_j(0)$ is the surface production rate of nuclide j. The decay constants λ_{10} and λ_{26} are 4.59 x 10^{-7} and 9.78 x 10^{-7} yr^{-1}, respectively, which correspond to half-lives of 1.51 x 10^6 yr for ^{10}Be and 0.709 x 10^6 yr for ^{26}Al. Some other authors (for example, Partridge and others, 2003) use a different half-life of 1.34 x 10^6 yr for ^{10}Be (as well as a correspondingly different analytical standard), and the difference between these values is also the subject of active research; pending resolution of this ambiguity we use the most commonly accepted value. We disregard nuclide production by muons in equation (2) because, except in the case of very high erosion rates (which do not occur in the context of this work), it is unimportant relative to nuclide production by spallation near the surface.

The range of possible ^{10}Be and ^{26}Al concentrations that can be generated by equation (2) for all positive values of t_{exp} and ϵ define the so-called "simple exposure island." Lal (1991) describes this in detail. Figure 2A shows it graphically. Samples with nuclide concentrations that do not lie within the simple exposure island cannot be explained by surface exposure alone, but must have a complex exposure history that also includes long periods of burial. (Strictly, as the location of the simple exposure island is specific to the surface production rate at a particular site, samples that are exposed at the surface in one location, and then moved to another site where the production rate is lower, can lie outside the island corresponding to their present location without having been buried. However, this possibility does not become important in this paper.)

We now describe burial of a previously exposed sample. If a sample with some initial nuclide concentrations that developed during a previous period of exposure is buried, the subsequent nuclide concentrations are related to the burial duration as follows: For a quartz sample with concentration of nuclide j at the time of burial $N_{j,0}$ (atoms g^{-1}), the nuclide concentration $N_j(t_b)$, after burial duration t_b (yr), at a depth below the surface z (g cm^{-2}) is:

$$N_j(t_b) = N_{j,0}e^{-\lambda_j t_b} + \frac{P_j(z)}{\lambda_j}(1 - e^{-\lambda_j t_b}) \tag{3}$$

where $P_j(z)$ is the production rate (atoms g^{-1} yr^{-1}) of nuclide j at depth z. Here we have disregarded the effect of surface erosion because the change in nuclide production rates with depth is very small at large depths. We could not make this assumption for samples that were buried at only a few meters depth [for example, in dating river terraces: see Granger and Smith (2000) and Wolkowinsky and Granger (2004)].

If we measure both ^{26}Al and ^{10}Be in a single buried sample, we can write equation (3) for each nuclide. These equations yield three unknowns: the burial time t_b and the initial nuclide concentrations $N_{10,0}$ and $N_{26,0}$. With only two measurements (the concentrations of ^{26}Al and ^{10}Be), we must make additional assumptions to determine t_b uniquely. The assumptions that are commonly used to accomplish this are based on the idea that samples have only experienced a single period of surface exposure and/or steady erosion before burial, in which case equation (2) provides the needed relationships between ^{26}Al and ^{10}Be concentrations at the time of burial. Three examples of such assumptions follow.

First, for short exposure times ($< \sim$50,000 yr) or high erosion rates ($> \sim$0.003 g cm^{-2} yr^{-1}) we can disregard radioactive decay, in which case the ^{10}Be and ^{26}Al concentrations in a surface sample are related by

$$\frac{N_{26}}{N_{10}} = R_0 \tag{4}$$

where R_0 is the production ratio. $R_0 = 6.1$ (Nishiizumi and others, 1989). This relation between the initial concentrations of ^{26}Al and ^{10}Be would allow us to calculate both the initial nuclide concentrations and the burial time t_b from ^{10}Be and ^{26}Al measurements on a buried sample.

Second, we can follow Granger and others (1997, 2001) and Partridge and others (2003), who dated samples of fluvial sediment deposited in caves. They assumed that their samples were derived from surfaces that had been continuously exposed for long enough that surface nuclide concentrations had reached a steady-state balance between production and loss by erosion and radioactive decay. In this case, the initial nuclide concentrations at the time of burial are related by:

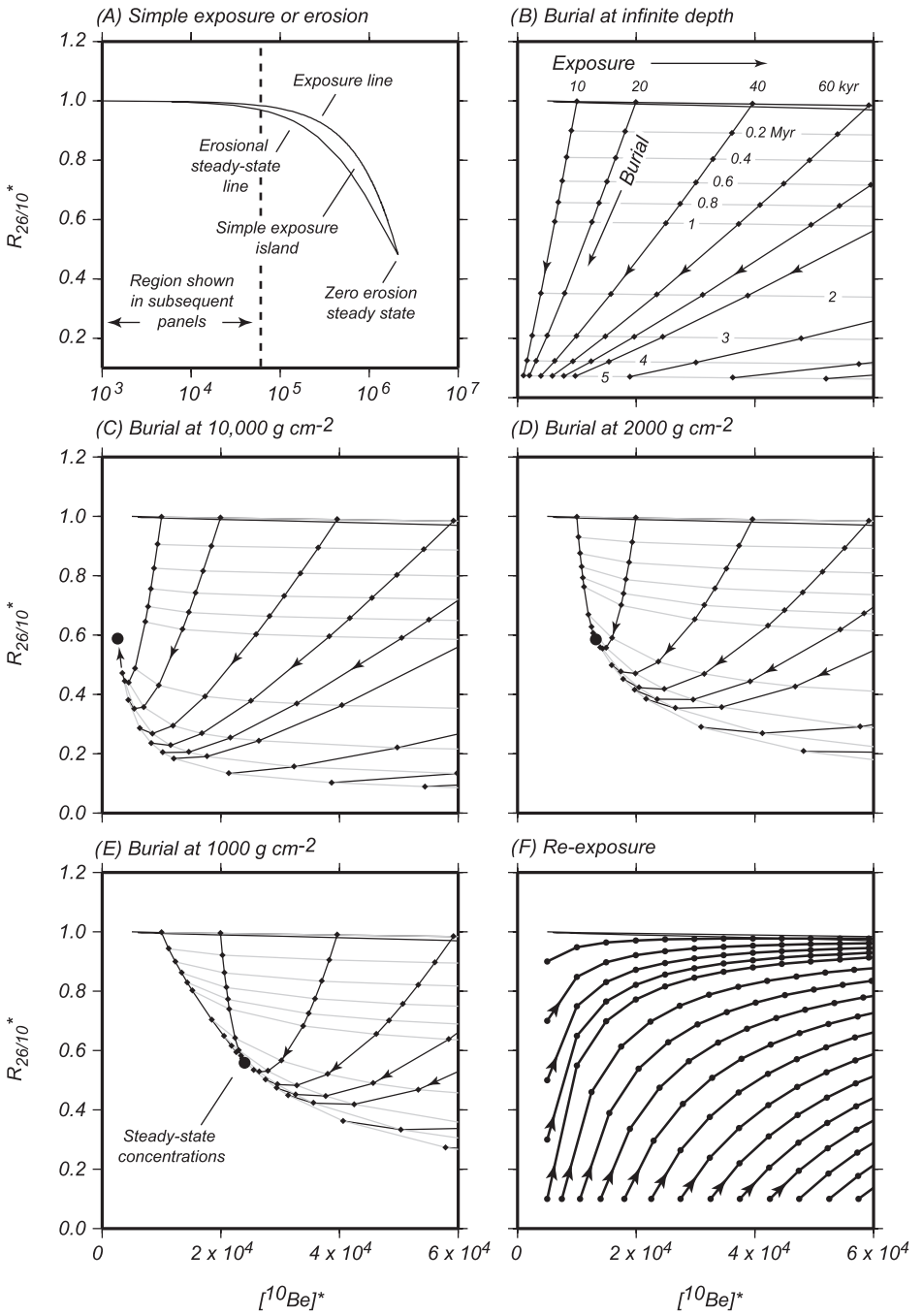

Fig. 2. Effect of surface exposure, burial, and re-exposure on ^{10}Be and ^{26}Al concentrations. In this and subsequent diagrams, the superscripted star indicates that measured nuclide concentrations have been normalized to the surface production rates of each nuclide. That is, $[^{10}Be]^* = N_{10}/P_{10}(0)$, where N_{10} is the measured concentration of ^{10}Be (atoms g^{-1}) and $P_{10}(0)$ is the surface production rate of ^{10}Be at the sample location (atoms g^{-1} yr^{-1}). $[^{10}Be]^*$ has units of yr. The normalized ^{26}Al/^{10}Be ratio $R^*_{26/10}$ is equal to R/R_0, where R is the measured ^{26}Al/^{10}Be ratio in a sample and R_0 is the surface production ratio ($R_0 = 6.1$). (A) The simple exposure island of Lal (1991), that is, the region of nuclide concentrations consistent with surface exposure that can be generated by equation (2). (B) Nuclide concentrations expected after a single

$$\left[\frac{P_{26}(0)\Lambda_{sp}}{N_{26}} - \lambda_{26}\Lambda_{sp}\right] = \epsilon = \left[\frac{P_{10}(0)\Lambda_{sp}}{N_{10}} - \lambda_{10}\Lambda_{sp}\right] \quad (5)$$

where $P_j(0)$ is the surface production rate, and ϵ is the erosion rate, at the location where the sample originated. In effect this relationship parameterizes the initial nuclide concentrations $N_{10,0}$ and $N_{26,0}$ in terms of the erosion rate ϵ. Thus, both ϵ and t_b are single-valued functions of the ^{26}Al and ^{10}Be measurements in a buried sample. Granger and Muzikar (2001) give formulae for this calculation. Note that in this case, as the next, we must specify the surface production rates during the initial exposure. For sediments whose source is not well known, this assumption contributes some uncertainty to ϵ, but in most cases does not significantly affect the value of t_b that we eventually determine.

Third, we can assume that the samples originated from a surface that was continuously exposed, without any erosion, for a time t_{exp}. In this case, the relationship between the initial nuclide concentrations is:

$$\left[\frac{-1}{\lambda_{26}}\ln\left(1 - \frac{N_{26}\lambda_{26}}{P_{26}(0)}\right)\right] = t_{\text{exp}} = \left[\frac{-1}{\lambda_{10}}\ln\left(1 - \frac{N_{10}\lambda_{10}}{P_{10}(0)}\right)\right] \quad (6)$$

that is, we parameterize $N_{10,0}$ and $N_{26,0}$ in terms of the exposure time t_{exp}, and we can then calculate t_{exp} and the burial time t_b from the two measurements.

Many authors have described this procedure graphically instead of mathematically (for example, Lal, 1991; Bierman and others, 1999). In graphical form, equation (4) above is equivalent to assuming that nuclide concentrations at the time of burial are restricted to the extreme "left side" of the simple exposure island in figure 2A. Equations (5) and (6) above are equivalent to assuming that nuclide concentrations at the time of burial are restricted to the "lower" and "upper" boundaries of the simple exposure island, respectively. Having made one of these assumptions, one can then use equation (3) to draw isolines of the erosion rate and burial time, or the exposure time and burial time, corresponding to any measured nuclide concentrations. In figure 2B-2E we provide isolines of exposure time and burial time drawn with the assumption that equation (6) holds at the time of burial. The form of this diagram varies depending on the depth of burial and thus the production rate during the period of burial; this means that the burial depth determines the age resolution that can be attained given a certain analytical precision.

One more possible scenario, which we discuss later in this paper, concerns a sample which has been exposed for a time, buried at a lower production rate for a time, and then re-exposed at the surface, that is, a sample which is brought to the surface with nuclide concentrations well outside the simple exposure island. Equation (3) applies in this case as well, and the nuclide concentrations in the sample will asymptotically approach the simple exposure island along the re-exposure trajectories shown in figure 2F.

The important points of this section are as follows:

---

period of surface exposure and a single period of burial at infinite depth. Dark lines show burial trajectories; light lines show burial isochrons. Note change from semi-logarithmic to linear axes. (C), (D), and (E), burial trajectories and isochrons for a single period of surface exposure and a single period of burial at 10,000, 2000, and 1000 g cm^{-2} respectively. Black circles denote steady-state nuclide concentrations at the respective depths. We used subsurface production rates generated with the Wyangla quarry muon interaction cross-sections (fig. 1) to construct these diagrams. (F) Re-exposure trajectories. If a sample with nuclide concentrations outside the simple exposure island is re-exposed at the surface, its nuclide concentrations will progress upward and to the right along the dark lines. Black dots indicate 5000-yr increments of exposure time.

1. If the measured ^{26}Al and ^{10}Be concentrations in a sample fall "below" the simple exposure island defined by the surface production rates $P_j(0)$ at the location they were originally exposed, that is,

$$\left[\frac{P_{26}(0)}{N_{26}} - \lambda_{26}\right] > \left[\frac{P_{10}(0)}{N_{10}} - \lambda_{10}\right] \quad (7)$$

   then the history of the sample must include burial as well as surface exposure. In the rest of this paper, we use the phrase "inconsistent with surface exposure" to describe this situation.
2. If we make at least one of the assumptions in equations (4)-(6) about the relationship of ^{26}Al and ^{10}Be concentrations at the time of burial, we can calculate the duration of burial (as well as one additional parameter) from measured ^{26}Al and ^{10}Be concentrations.

^{26}Al/^{10}Be Dating of Buried Sediments in Complicated Situations

In effect the procedure that we describe above treats equation (3) as a predictive model that tells us the nuclide concentrations we expect in the sample as a function of the unknown parameters $N_{26,0}$, $N_{10,0}$, and t_b. We then seek the values of these parameters that best predict the nuclide concentrations we actually measure. For a single sample, the number of parameters (3) exceeds the number of measurements (2), so we use the assumptions in equations (4), (5), and (6) to reduce the number of unknowns to equal the number of measurements. The unknown parameters are then single-valued functions of the measurements, and can be found by relatively simple analytical formulae.

The difficulty with this approach, in which we make assumptions to reduce the number of unknown parameters, is that these assumptions are only valid in very restricted geological situations. Fluvial sediments that originate from a slowly eroding landscape and are deposited in caves are one of these. In general, however, we expect that sediments in many environments will have already had a complicated exposure history, including many periods of exposure, burial, erosion, transportation, and redeposition, before the final burial of interest, and that these assumptions will not be valid. In the first part of this paper (RESULTS AND DISCUSSION I: BURIED RIVER SANDS AND OUTWASH section), we show that this complicated history is true of fluvial sediments intercalated with tills in glacial sedimentary sequences: therefore we cannot use assumptions based on equation (2) to determine when these sediments were buried by overlying tills.

An alternative, to the simple approach of reducing the number of parameters by making convenient assumptions, is to collect more samples, whose exposure histories are somehow linked, and use this larger data set to determine a larger number of unknown parameters. In the second part of the paper (RESULTS AND DISCUSSION II: PRE-WISCONSINAN PALEOSOLS section), we use this approach to determine the burial age of paleosols developed on one till and then buried by subsequent units. We measure ^{26}Al and ^{10}Be concentrations in samples of quartz from various depths in the buried paleosol. These measured nuclide concentrations reflect the initial nuclide concentrations in the lower till at the time it was emplaced, the duration of near-surface exposure during soil development, and the duration of several periods of burial by successively increasing thicknesses of overburden. Thus, an exposure model that we use to predict the present nuclide concentrations in our samples has several parameters: the initial nuclide concentrations in quartz in the lower till, and the lengths of exposure and burial periods. We use whatever geological data are available to estimate some of these parameters independently, and then use a numerical optimization method (rather than the analytical solutions we can use in the simple

method) to determine the values for the remaining parameters that best explain the measured nuclide concentrations.

The mathematical description of this procedure is as follows. In the most general sense, what we are doing is solving the basic differential equation for nuclide production and decay:

$$\frac{dN}{dt} = P(z(t)) - \lambda N \tag{8}$$

where the function $P(z)$ reflects the depth dependence of the production rate. We want to determine the age/depth function $z(t)$, which encapsulates the ages or durations of whatever geologic events we are interested in. If we can use the geological context of the sample to suggest a form for $z(t)$ that has a manageable number of unknown parameters, we can then seek best-fitting values for these parameters. In effect we are using geologic information to answer the question "what happened," and then using cosmogenic-nuclide measurements to answer the questions "when," or "how fast."

For our specific case of paleosols buried by a series of stratified sediments, where the samples are buried deeply enough that we can disregard surface erosion, the age/depth history $z(t)$ resembles a step function. We can extend equation (3) to describe this case for multiple samples and multiple nuclides by denoting the concentration of nuclide j in sample i at the end of time period k by $N_{i,j,k}$. The subscripts k go from $1 \ldots K$ where K is the total number of exposure or burial periods in the sample history. Then,

$$N_{i,j,k} = N_{i,j,(k-1)} e^{-\lambda_j t_k} + \frac{P_j(z_{i,k})}{\lambda_j} (1 - e^{-\lambda_j t_k}) \tag{9}$$

where $P_j(z_{i,k})$ is the production rate of nuclide j at depth $z_{i,k}$, the depth of sample i during time period k. For multiple samples from a paleosol that experiences surface exposure during period $k=1$, the depths $z_{i,1}$ are the depths of the samples below the paleosol surface. For the periods of burial where $k > 1$, the depths $z_{i,k} = z_{i,1} + Z_k$ where Z_k is the depth of overburden covering the soil surface during period k. The depths of the samples below the present land surface are $z_{i,K} = z_{i,1} + Z_K$. We start with initial nuclide concentrations at the beginning of the first time period $N_{i,j,0}$ and apply this equation K times to arrive at the final nuclide concentrations $N_{i,j,K}$.

We can estimate the production rates during the different time periods $P_j(z_{i,k})$ from the present stratigraphy and the depth dependence of nuclide production rates. Some of the durations of exposure or burial periods t_k may be known from correlation to nearby units or other age information, and some are unknown. The initial nuclide concentrations $N_{i,j,0}$ are in most cases unknown. To summarize, this yields a predictive model for the final nuclide concentrations $N_{i,j,K}$ as a function of one or more unknown parameters, usually the initial nuclide concentrations and the durations of the various periods of burial. We then use standard mathematical optimization methods to select the parameters that minimize the difference between predictions and actual measurements. Balco and others (2005) describe this approach, its assumptions, and the optimization method in more detail.

THE STRATIGRAPHIC RECORD OF PLIO-PLEISTOCENE ADVANCES OF THE LAURENTIDE ICE SHEET

The former location of the Laurentide Ice Sheet is today delimited by a broad arc of exposed, lake-riddled, and glacially scoured Precambrian bedrock surrounded by an outer zone near the past ice margin where thick sequences of glacial sediment have been deposited. Here we are interested in the portion of this arc of deposition within

the north-central United States (fig. 3). In northernmost Minnesota, the glacial section consists only of thin deposits of the last glaciation overlying eroded bedrock. Glacial deposits thicken to the south, and eastern South Dakota, southwestern Minnesota, and western Iowa are covered by up to 250 m of Plio-Pleistocene glacial sediment, which consists mostly of laterally extensive till sheets interbedded with fluvial or glaciofluvial sediment. Paleosols and loess are rare in this region. Farther south, in southern Iowa, eastern Nebraska, and Missouri, the total glacial section is thinner, fewer till sheets are present, tills are separated by well-developed paleosols, and loess is common. It appears that the northernmost part of the region experienced mostly glacial erosion, and areas south of central Minnesota experienced deposition of till and ice-marginal sediment during nearly all ice advances. The area of thickest sediment in southwest Minnesota, where the largest number of tills is present, likely experienced numerous and relatively frequent glaciations; the southernmost glaciated regions experienced fewer glaciations and longer intervening periods (Boellstorff, 1978c; Hallberg, 1986; Hallberg and Kemmis, 1986; Setterholm, 1995; Patterson, 1997, 1999; Soller and Packard, 1998; Roy and others, 2004). Here we focus on two areas: the region of thickest glacial sediment in southwestern Minnesota and adjacent South Dakota, and the region of thinner sediment, fewer tills, and better-developed interglacial deposits in eastern Nebraska and adjacent Iowa (fig. 3).

Southwestern Minnesota and Adjacent South Dakota

The thickest sequences of Pleistocene tills in the north-central U.S. occur beneath the Prairie Coteau highland near the Minnesota-South Dakota border. Here multiple till sheets are interbedded with sands and silts that record either ice-marginal glaciofluvial and glaciolacustrine deposition or fluvial systems that existed during interglaciations. Individual boreholes penetrate up to 12 distinct tills, indicating that at least this number of ice sheet advances took place. Some boreholes that reach bedrock penetrate mature quartz sands containing charcoal, woody plant debris, and mammal bones and teeth, suggesting a lowland riverine environment that predates Pleistocene glaciation. Gilbertson and Lehr (1989), Lineburg (ms, 1993), Setterholm (1995), and Patterson (1997), describe this stratigraphy.

The age of these tills is uncertain. The lower part of the section is correlated with magnetically reversed sediments, indicating that at least some ice advances occurred prior to 0.78 Ma (Patterson, 1997). The Lava Creek B ash (0.6 Ma) occurs between tills somewhat to the west (Flint, 1955), but correlation from this site into our study area is uncertain. Wisconsinan ice covered only the edges of the Prairie Coteau.

The Minnesota River lowland to the northeast of the Prairie Coteau also contains a thick sequence of tills. These tills are associated with the Des Moines lobe of the Laurentide Ice Sheet and are generally of northwestern provenance. Here several Wisconsinan tills at the surface are underlain by at least five distinct pre-Wisconsinan tills. These form at least two unconformity-bounded packages, each of which presumably records a single glacial-interglacial cycle. These packages are separated by laterally extensive, linear sand units apparently deposited by well-developed interglacial fluvial systems. The age of these tills is unknown, and correlations between the Minnesota River Valley and Prairie Coteau sections are likewise uncertain. Patterson (1999) describes this stratigraphy.

Eastern Nebraska and Adjacent Iowa

Boellstorff (1978a, 1978b, 1978c) and Roy and others (2004) describe the sequence of tills in eastern Nebraska and adjacent Iowa. The earliest of these tills, the "C" tills of Boellstorff and the "R2" tills of Roy and others, consist of at least two tills that have distinctive clay mineralogy, are magnetically reversed, and underlie the 2.0 Ma Huckleberry Ridge ash. The "B" tills of Boellstorff (1978c) ["R1" in Roy and others

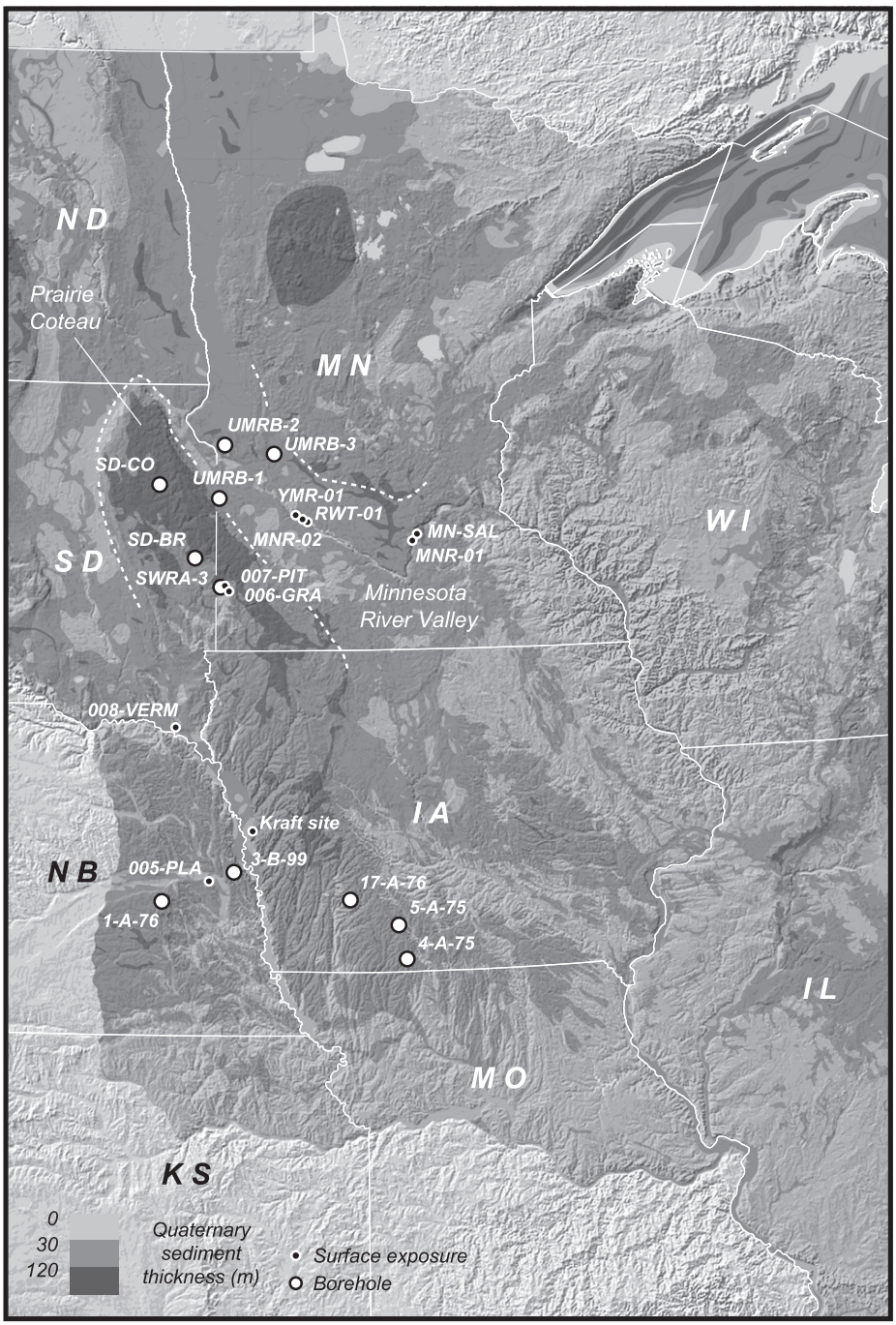

Fig. 3. Locations of boreholes and other samples discussed in text. Background shows shaded relief overlain by total Quaternary sediment thickness, for areas within the U.S., from Soller and Packard (1998).

TABLE 1

Locations and nuclide production rates for boreholes and excavations mentioned in text. Production rates calculated according to Stone (2000).

Designation (in this work)	Latitude	Longitude	Wellhead elevation (m)	Nuclide production rates in quartz at surface (atoms g^{-1} yr^{-1}) ^{10}Be	^{26}Al	Reference
UMRB-1	44.8970 N	96.4125 W	358	6.9	42.3	Patterson (1999)
UMRB-2	45.3823 N	96.3467 W	335	6.8	41.7	Patterson (1999)
UMRB-3	45.3012 N	95.7066 W	334	6.8	41.6	Patterson (1999)
SWRA-3	44.0821 N	96.3888 W	529	8.0	48.6	Setterholm (1995)
SD-BR	44.3478 N	96.7175 W	507	7.8	47.9	Lineburg (ms, 1993)
SD-CO	45.0186 N	97.1847 W	547	8.2	49.9	S.D. Geol. Surv., unpub. data
4-A-75	40.6819 N	94.1144 W	347	6.6	40.1	Boellstorff (1978a)
5-A-75	40.9983 N	94.2000 W	354	6.6	40.5	Boellstorff (1978a)
1-A-76	41.2225 N	97.0992 W	494	7.5	45.7	Boellstorff (1978a)
17-A-76	41.2303 N	94.7936 W	396	6.9	42.1	Boellstorff (1978a)
3-B-99	41.4908 N	96.2129 W	398	6.9	42.3	Mason (2001)
Kraft site	41.8616 N	95.9925 W	332	6.6	40.1	Bettis (1990)

(2004)] comprise at least two tills that are magnetically reversed and overlie the 1.3 Ma Mesa Falls ash, suggesting deposition between 1.3 Ma and 0.78 Ma. The uppermost set of tills ["A" tills of Boellstorff (1978c); "N" of Roy and others (2004)] comprises at least three tills that have normal magnetic polarity. At least one of these is younger than the 0.6 Ma Lava Creek B ash. Wisconsinan ice did not cover this region. Thick sand units are rare. Surfaces of individual tills are commonly oxidized or weathered, and often exhibit well-developed paleosols, suggesting long periods of exposure between ice advances. The uppermost till is commonly covered by one or more loess units separated by paleosols. The uppermost two loess units, designated the Peoria and Loveland formations in eastern Nebraska, were deposited 35,000 to 12,000 yr B.P. and 150,000 to 135,000 yr B.P. respectively (Forman and others, 1992; Forman and Pierson, 2002). The age of loess units below these uppermost two is unknown. Borehole locations and nuclide production rates for boreholes and excavation localities discussed in this study are listed in table 1.

ANALYTICAL METHODS

Quartz Separation and Al/Be Extraction

We disaggregated samples of till, sand, silt, and soil by drying, crushing, soaking in water, KOH, HNO_3, or $(NaPO_3)_6$ ("Calgon"), ultrasonic bath treatment, or some combination thereof, then isolated the appropriate grain size by wet-sieving. In most cases we used the 0.25 to 0.85 mm grain size, but for small samples we used material as fine as 0.125 mm in order to obtain sufficient quartz. ^{26}Al and ^{10}Be analyses of separate coarse (0.25 - 0.85 mm) and fine (0.125 - 0.25 mm) grain-size fractions for samples of outwash (two samples) and till (one sample) were indistinguishable, as expected for glacial sediment, which is likely to be immature, well-mixed, and poorly sorted. We extracted and purified quartz by repeated etching in 2 percent HF, heavy-liquid separation to remove acid-insoluble heavy minerals, soaking in hot KOH to remove

secondary fluoride precipitated during the HF treatment, and a final 2 percent HF etch. This procedure yielded quartz with 35 to 80 ppm Al. We extracted Al and Be from 25 to 35 g of quartz using standard methods (Ditchburn and Whitehead, 1994; Stone, 2004), prepared Al cathodes by Al/Ag coprecipitation (Stone and others, 2004), and measured isotope ratios at the Lawrence Livermore National Laboratory, Center for Accelerator Mass Spectrometry.

Our combined process and carrier blanks were $6.3 \pm 6.5 \times 10^4$ atoms ^{26}Al, $2.6 \pm 2.5 \times 10^4$ atoms ^{10}Be for analyses conducted in 2002, and $2.6 \pm 0.3 \times 10^5$ atoms ^{10}Be for analyses conducted in 2003. Although process blanks run simultaneously with samples in 2003 yielded repeatable results at the level noted above, we discovered later that at least some of the aluminum metal cathodes used to hold BeO samples for AMS analysis during 2003 contained large quantities of ^{10}Be ($> 3 \times 10^7$ atoms $g(Al)^{-1}$)). Sputtering of exposed Al metal during AMS analysis probably contributed spurious ^{10}Be counts to some samples that are not fully reflected in the process blank measurements. Thus, it is likely that we have under corrected a small, but unknown, number of our ^{10}Be measurements. We discuss the results that may have been affected by this under-correction later in the text.

Density Measurements

In order to estimate subsurface nuclide production rates at our sample sites, we measured the density of 132 samples from our set of drillcores. For a few samples of non-cohesive sand and silt, we measured density by packing a container of known volume to approximate the natural compaction of the material. The majority of the samples consisted of irregular blocks of till or weakly cemented sand and silt. We measured their density by an adaptation of the procedure outlined by Sheldrick (1984) (also see Balco, 2004a). We weighed each sample, placed it in a container of known volume, filled the remainder of the container with 1-mm glass beads, and weighed sample, container, and beads. Having already measured the density of packed glass beads, we could subtract the volume of beads from the volume of the container to determine the volume of the sample and thence the density. By repeatedly measuring the density of quartz ($\rho = 2.65$ g cm^{-3}) samples, we determined the accuracy of this procedure to be ± 0.08 g cm^{-3}.

The drillcore samples available to us had been air-dried to atmospheric moisture content during 3 to 30 yr of storage. However, the units we sampled, and nearly all of their overburden, are actually water-saturated in the field, and were most likely water-saturated during most of their history. Thus, we require their wet density in order to calculate shielding depths. We inferred the wet density of samples by assuming that the dried sample consisted entirely of quartz grains: if such a sample were fully water-saturated, the wet density would be:

$$\rho_{wet} = \left(1 - \frac{\rho_{dry}}{\rho_{quartz}}\right) + \rho_{dry} \tag{10}$$

where ρ_{dry} is the dry density of the sample and ρ_{quartz} is the density of quartz (2.65 g cm^{-3}). We evaluated this assumption by measuring wet and dry densities for the following: a) naturally water-saturated samples of till collected at outcrops and mine excavations that we then dried, and b) dry drillcore samples of sand, silt, and till that we then saturated with distilled water. We found that measured wet densities for both naturally wet samples and saturation experiments coincided with those calculated using equation (10) within measurement error (fig. 4).

For units whose density we did not actually measure, we assigned the average density measured for other samples of the same type of sediment. These average wet bulk densities are 2.24 ± 0.07 g cm^{-3} for till ($n = 90$), 2.13 ± 0.16 g cm^{-3} for sand ($n =$

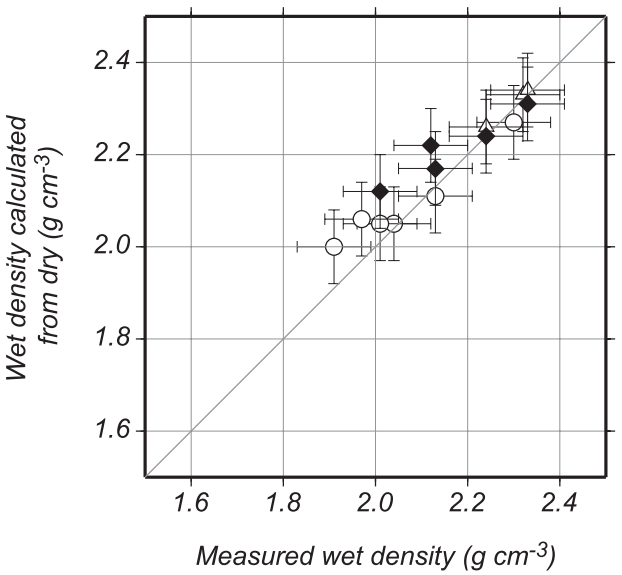

Fig. 4. Comparison of measured wet bulk densities, with wet densities calculated from dry density measurements using equation (10). Open circles, unconsolidated sand collected dry from drill core and then resaturated. Solid diamonds, till collected wet in the field and then dried. Open diamonds, till collected dry from drill core and then resaturated.

35), and 2.01 ± 0.1 g cm^{-3} for glaciolacustrine silts (n = 7). We assigned compacted loess a wet density of 2.3 g cm^{-3} based on measurements by J. Mason (personal communication).

If we take into account the analytical errors in density measurements, density variability within units, and our assumption that most units are permanently water-saturated, we estimate that we can only estimate the long-term shielding depth of most samples to within approximately 10 percent. The importance of this uncertainty to our eventual results depends on the burial depth of samples: the greater the burial depth, the less important the uncertainty in the shielding depth. In most of the examples we discuss in this paper, uncertainty in the density measurements is relatively unimportant, and we do not consider it further. Balco and others (2005) provide a more detailed error analysis.

Results and discussion I: buried river sands and outwash

In this paper we report results of ^{26}Al and ^{10}Be analyses of two types of glacial sediment: first, sandy fluvial sediment and outwash intercalated with tills; and second, paleosols developed on tills and then buried by other glacial sediment. In this first section we discuss fluvial sediment and outwash. We discuss paleosols in the next section.

The buried fluvial and glaciofluvial sands whose burial age we wish to determine consist of fine sand to gravel interbedded with till in five boreholes from southwest Minnesota and adjacent South Dakota (figs. 3, 5). These sand units are up to 20 m thick and, in many cases, can be correlated between drillholes to reveal channel networks that record river systems developed during interglacial periods (Patterson, 1999). The reason we became interested in these sands at first is that nearly all modern river sands for which ^{26}Al and ^{10}Be have previously been measured have nuclide concentrations that comply with equation (5) (Granger and others, 1996, 1997, 2001; Clapp and others, 2000; Partridge and others, 2003; Stock and others, 2004). Thus, we thought that we could use the simple approach previously described in the *^{26}Al/^{10}Be*

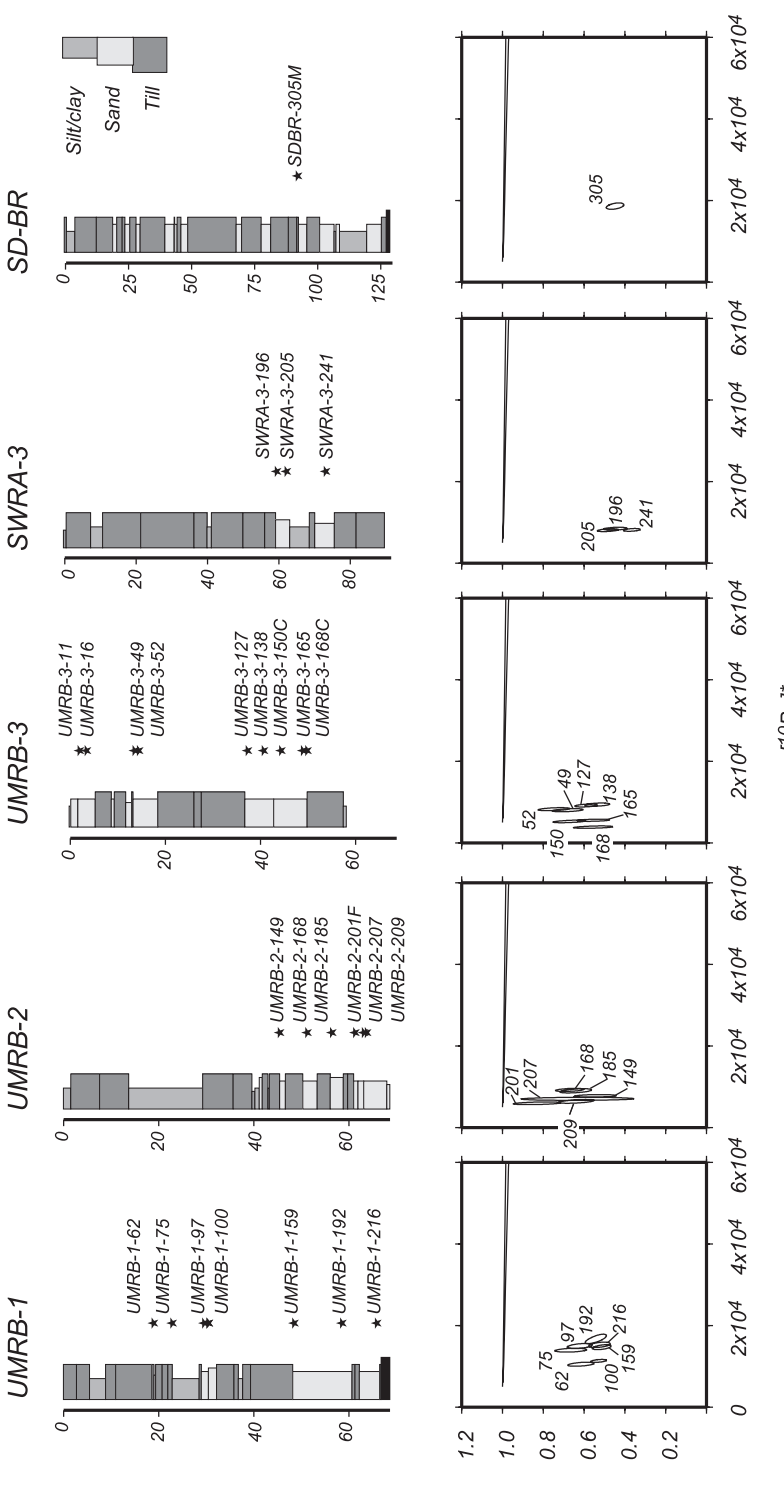

Fig. 5. Stratigraphic context of pre-Wisconsinan fluvial sand and outwash samples. Stars and accompanying sample names indicate locations of samples in boreholes. In this and all following ^{10}Be – $^{26}Al/^{10}Be$ diagrams, we use 68% confidence ellipses to show ^{10}Be and ^{26}Al concentrations in each sample. Lower panels show ^{10}Be and ^{26}Al concentrations on the same axes as figs. 2B-2F. Fig. 3 shows location of boreholes.

TABLE 2

^{26}Al and ^{10}Be concentrations in pre-Wisconsinan fluvial sands and outwash in boreholes. In this and subsequent tables, ^{10}Be concentrations are reported relative to LLNL internal standards, which are traceable to the ICN ^{10}Be standard. ^{26}Al concentrations are reported relative to LLNL internal standards. Uncertainties are reported at ±1 σ and include all known sources of analytical error. Blank corrections are described in the text.

Sample name	Borehole	Depth (m)	[^{10}Be] (10^4 atoms g^{-1})	[^{26}Al] (10^4 atoms g^{-1})
UMRB-1-62	UMRB-1	18.9	7.30 ± 0.23	27.4 ± 1.7
UMRB-1-75	UMRB-1	22.9	9.69 ± 0.22	39.3 ± 3.1
UMRB-1-97	UMRB-1	29.6	10.35 ± 0.29	39.4 ± 2.4
UMRB-1-100*	UMRB-1	30.5	7.87 ± 0.17	25.4 ± 1.1
UMRB-1-159	UMRB-1	48.5	10.19 ± 0.28	31.9 ± 1.7
UMRB-1-192	UMRB-1	58.5	11.60 ± 0.55	38.3 ± 1.8
UMRB-1-216	UMRB-1	65.9	10.56 ± 0.31	33.9 ± 2.1
UMRB-2-149	UMRB-2	45.4	5.30 ± 0.16	17.6 ± 2.3
UMRB-2-168	UMRB-2	51.2	6.31 ± 0.18	25.8 ± 1.7
UMRB-2-185	UMRB-2	56.4	6.15 ± 0.24	24.0 ± 1.7
UMRB-2-201F	UMRB-2	61.3	4.07 ± 0.15	20.6 ± 1.8
UMRB-2-207	UMRB-2	63.1	4.81 ± 0.18	18.5 ± 5.7
UMRB-2-209	UMRB-2	63.7	4.38 ± 0.23	17.0 ± 1.4
UMRB-3-49	UMRB-3	14.9	5.54 ± 0.18	22.5 ± 1.5
UMRB-3-52	UMRB-3	15.9	5.64 ± 0.17	25.7 ± 1.6
UMRB-3-127	UMRB-3	38.7	6.25 ± 0.16	22.5 ± 1.3
UMRB-3-138	UMRB-3	42.1	6.4 ± 0.19	20.9 ± 1.5
UMRB-3-150C	UMRB-3	45.7	3.59 ± 0.14	14.7 ± 1.0
UMRB-3-165	UMRB-3	50.3	3.79 ± 0.13	12.8 ± 1.2
UMRB-3-168C	UMRB-3	51.2	2.64 ± 0.14	8.9 ± 1.0
SWRA-3-196	SWRA-3	59.8	6.74 ± 0.19	18.4 ± 1.5
SWRA-3-205	SWRA-3	62.5	6.45 ± 0.19	19.0 ± 1.3
SWRA-3-241	SWRA-3	73.5	6.5 ± 0.19	14.6 ± 1.1
SDBR-305M	SD-BR	93.0	14.64 ± 0.42	39.9 ± 2.3
SD-CO-402	SD-CO	122.6	13.89 ± 0.40	35.4 ± 2.8
SD-CO-406	SD-CO	123.8	12.49 ± 0.53	38.2 ± 2.3

*Mean of two analyses

Dating of Buried Sediments in Simple Situations section to determine the time that these sediments were buried by overlying tills, and thus the age of the tills. However, we found that this was not the case, and that we could not constrain the initial nuclide concentrations in these sediments at the time they were buried. In this section we describe the reasoning that led us to this conclusion and summarize the limited age information that we could obtain from our measurements.

We measured ^{26}Al and ^{10}Be in 33 samples from these buried sand units (fig. 5; table 2). Many of these samples belonged to the thick, laterally extensive, and well-sorted sand units deposited by river systems that developed during interglaciations, and others belonged to thinner, less extensive, and less well-sorted sands that could have been rapidly deposited near the ice margin. We observed no systematic difference between samples from these two stratigraphic contexts. We found that $^{26}Al/^{10}Be$ ratios decreased with depth in nearly all cases, that $^{26}Al/^{10}Be$ ratios of correlative sand units from different boreholes agreed, and that nuclide concentra-

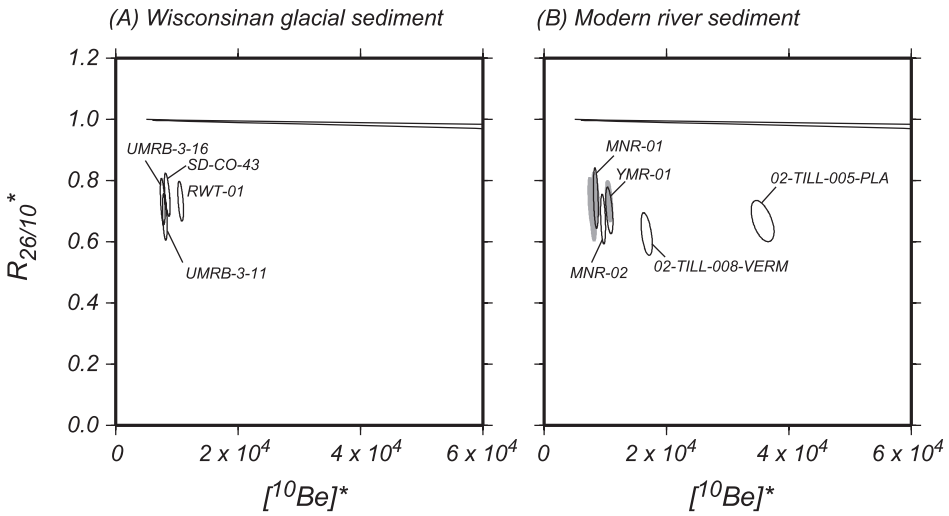

Fig. 6. (A) ^{26}Al and ^{10}Be concentrations in Wisconsinan glacial sediment from southwest Minnesota and adjacent South Dakota. UMRB-3-11 and -16 are samples of glaciolacustrine sand and silt from borehole UMRB-3; RWT-01 is a sample of sandy outwash from a terrace of the glacial River Warren; and SD-CO-43 consists of quartz extracted from the uppermost till in borehole SD-CO. Fig. 3 shows sample locations. (B) ^{26}Al and ^{10}Be concentrations in modern river sands. Fig. 3 shows sample locations. Data from (A) are reproduced in gray to highlight the close agreement between nuclide concentrations in Wisconsinan glacial sediment and modern river sand from the Minnesota River Valley. Measured nuclide concentrations in this figure have been normalized to typical regional surface production rates of 7 and 42.5 atoms g^{-1} yr^{-1} for ^{10}Be and ^{26}Al respectively.

tions in buried sands were near expected values for sediments that had experienced 10,000 to 50,000 yr of surface exposure and 0.5 to 1.5 Myr of burial below several meters depth. The fact that we obtained plausible results, did not infer age reversals, and did not violate stratigraphic constraints suggested at first that we were justified in assuming that ^{26}Al and ^{10}Be concentrations at the time of burial were consistent with surface exposure.

Results From Modern Fluvial Systems

In order to better evaluate our assumptions about ^{10}Be and ^{26}Al concentrations at the time of burial, we measured ^{26}Al and ^{10}Be concentrations in samples of sand being transported in modern rivers (fig. 6; tables 3, 4; sample locations shown in fig. 3). We

Table 3

Location of samples of modern river sediment and Wisconsinan glacial deposits.

Sample name	Latitude	Longitude	Elevation (m)	Description
RWT-01	44.6750 N	95.2828 W	306	Gravel pit near Granite Falls, MN, in terrace of glacial River Warren
MNR-01	44.5297 N	95.9019 W	218	Channel of Minnesota River
MNR-02	44.6950 N	95.3403 W	261	Channel of Minnesota River
YMR-01	44.7389 N	95.4294 W	264	Channel of Yellow Medicine River
02-TILL-005-PLA	41.4092 N	96.5176 W	365	Channel of Platte River
02-TILL-008-VERM	42.8033 N	96.9509 W	361	Channel of Vermilion River

TABLE 4

^{26}Al and ^{10}Be concentrations in modern river sands.

Sample name	[^{10}Be] (10^4 atoms g^{-1})	[^{26}Al] (10^4 atoms g^{-1})	Description
MNR-01	5.15 ± 0.17	23.3 ± 2.0	Minnesota River, MN
MNR-02	6.11 ± 0.18	25.1 ± 2.0	Minnesota River, MN
YMR-01	6.78 ± 0.25	29.0 ± 1.8	Yellow Medicine River, MN
02-TILL-005-PLA	24.02 ± 0.84	97.6 ± 5.6	Platte River, NB
02-TILL-008-VERM	11.42 ± 0.42	43.4 ± 2.8	Vermilion River, SD

found that nuclide concentrations in these samples are not consistent with surface exposure. We also measured ^{26}Al and ^{10}Be concentrations in subsurface samples from tills and ice-marginal deposits of latest Wisconsinan age (fig. 6; table 5). Nuclide concentrations in sand from the modern Minnesota River and its tributaries (samples MNR-01, MNR-02, YMR-01) were indistinguishable from those in Wisconsinan glacial sediments deposited by the Des Moines lobe. If this modern river sand was derived from slow erosion of nearby soil surfaces that had been exposed to the cosmic ray flux since deglaciation 15,000 yr ago, it would have higher ^{26}Al and ^{10}Be concentrations than Wisconsinan glacial sediments that had remained buried since emplacement. The fact that these higher concentrations are not observed shows that most of the sediment in the river systems is derived from rapid undermining of steep riverbank bluffs that expose glacial deposits, rather than from gradual erosion of soil surfaces over large areas. The remarkable agreement of nuclide concentrations in latest Wisconsinan glacial sediment from a variety of environments, all ultimately derived from subglacial erosion of older glacial sediments, also indicates that the last ice sheet advance was very effective in mixing and homogenizing the sediment that it transported. Thus, the Wisconsinan advance of the Des Moines lobe into the Minnesota River valley mobilized, mixed, and redeposited older glacial sediment that already had experienced an exposure/burial history of at least 500,000 yr, and this sediment is now moving directly into rivers without being measurably exposed to the surface cosmic ray flux. If modern river sands were buried by future glacier advances and we subsequently attempted to calculate their burial age by assuming that nuclide concentrations were consistent with surface exposure at the time of burial, we would obtain wildly incorrect ages.

TABLE 5

^{26}Al and ^{10}Be concentrations in Wisconsinan glacial sediment in southwest Minnesota and adjacent South Dakota.

Sample name	[^{10}Be] (10^4 atoms g^{-1})	[^{26}Al] (10^4 atoms g^{-1})	Description
UMRB-3-11	5.47 ± 0.18	22.7 ± 1.6	Late Wisconsinan glaciolacustrine silt at 3.4 m in core UMRB-3
UMRB-3-16	5.23 ± 0.18	23.3 ± 1.4	Same, at 4.9 m depth
RWT-01	7.01 ± 0.20	31.3 ± 1.6	Late Wisconsinan outwash from terrace of glacial River Warren
SD-CO-43	6.88 ± 0.27	31.6 ± 1.6	Wisconsinan till at 13.1 m depth in borehole SD-CO

$^{26}Al/^{10}Be$ Ratios Below the Production Ratio in River Sands From Prior Interglacials?

If river sands in previous interglaciations had a similar history to modern river sands, we cannot assume that nuclide concentrations in these sands when they were buried by overlying tills were anywhere near consistent with surface exposure. Thus, we looked for further evidence that would tell us whether or not nuclide concentrations in pre-Wisconsinan river sediment were anything like those that we observe in modern river sands. First, we considered the possibility that recycling of older glacial sediment into the modern river system has been particularly pronounced in the Minnesota River Valley during the present interglaciation. The modern Minnesota River occupies a deep valley, cut through the entire glacial section by drainage from glacial Lake Agassiz, and tributary streams have incised several hundred feet of glacial sediment to reach the valley floor. However, we analyzed two samples of river sand from farther south and west (02-TILL-008-VERM from the Vermilion River in South Dakota and 02-TILL-005-PLA from the Platte River in Nebraska; see fig. 3) and found ^{26}Al and ^{10}Be concentrations that were different from Minnesota River samples, but were also inconsistent with surface exposure.

Direct measurements from buried sands of known age.—The ^{26}Al and ^{10}Be concentrations of modern river sediment show that nuclide concentrations that are inconsistent with surface exposure appear to be the rule for river sands in regions covered by glacial sediment in the present interglaciation. We evaluated whether or not this was the rule in previous interglaciations by collecting samples of middle Pleistocene fluvial sands whose burial ages were constrained by independent evidence, and back-calculating the nuclide concentrations in these samples at the time they were buried (fig. 7; table 6).

In borehole 4-A-75 (Boellstorff, 1978b), we sampled a coarse sand unit overlain by a normally magnetized till [the "A3" till of Boellstorff (1978b)] which was deposited 0.78 to 0.6 Ma. This till was overlain by loess containing the 0.6 Ma Lava Creek ash, and then by two pre-Wisconsinan tills ("A1" and "A2") that were emplaced 0.6 to 0.15 Ma (fig. 7). We estimated the nuclide concentrations in the sand at the time it was buried with a Monte Carlo simulation, as follows: We generated 1000 plausible burial histories by assuming that the loess unit was deposited 0.6 Ma, and selecting random ages for the other two units that were uniformly distributed between the age constraints. Then, for each of these permissible burial histories, we applied equation (3) repeatedly to back-calculate the initial ^{10}Be and ^{26}Al concentrations in the sample at the time of burial. This procedure yields the range of nuclide concentrations at the time of burial that are permitted by the constraints on the age of the overburden.

In borehole 1-A-76 (Boellstorff, 1978b), we sampled a sand unit that was overlain by a loess containing the 1.2 Ma Mesa Falls ash, by two tills (the "B2" and "A3" tills) that were deposited 1.2 to 0.6 Ma, and then by another sand unit that was deposited 0.6 to 0 Ma, and used the same procedure to estimate nuclide concentrations in the sample at the time of burial.

Figure 7 summarizes these results. Nuclide concentrations consistent with surface exposure at burial are not completely excluded for either sample, but are very unlikely in both cases.

At a gravel pit exposure in eastern Iowa (the Kraft locality of Bettis, 1990) we sampled sand and gravel, thought to be distal outwash from an ice margin somewhere to the northeast of the site, which contains the 0.6 Ma Lava Creek B ash (fig. 7; table 6). The samples are now buried under 6 to 10 m ($\sim$ 1200 - 2000 g cm^{-2}) of sand and loess, but field relationships show that this overburden has been eroded significantly. Thus, the burial history of these samples is poorly constrained. However, we can obtain a maximum limit for the $^{26}Al/^{10}Be$ ratio at the time of burial by assuming that the samples have been buried at infinite depth since the time of ash deposition, and applying equation (3). Figure 7 summarizes this calculation. Regardless of the burial

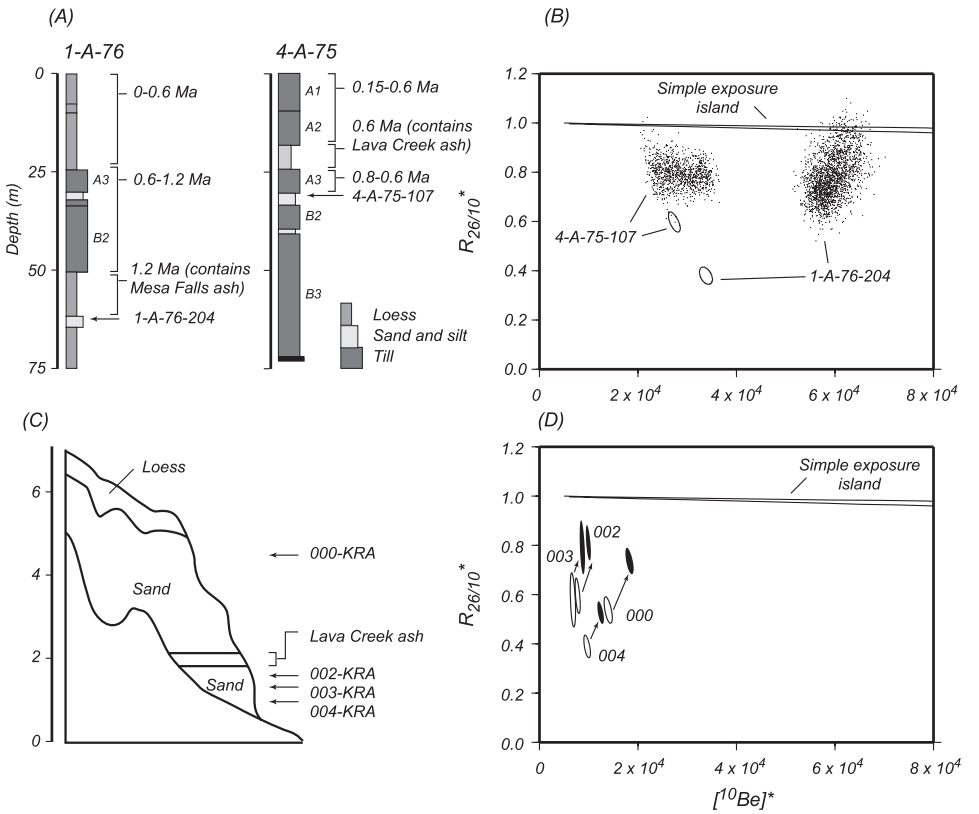

Fig. 7. ^{26}Al and ^{10}Be concentrations at time of burial inferred from samples of fluvial sediment of approximately known age. (A) Stratigraphy of boreholes 1-A-76 and 4-A-75 (Boellstorff, 1978a), showing age constraints on units overlying our samples. samples from boreholes 4-A-75 and 1-A-76. (B) Measured nuclide concentrations in samples (68% confidence ellipses) and possible nuclide concentrations at the time of burial (dots) generated from Monte Carlo simulation described in text. (C) Diagrammatic stratigraphy of Kraft exposure of Lava Creek ash showing sample locations relative to the ash (Bettis, 1990). (D) Measured nuclide concentrations in samples from Kraft site (unfilled ellipses) and inferred nuclide concentrations at the time of burial (filled ellipses), calculated as described in text.

depth, the ^{26}Al/^{10}Be ratio in these samples was well below the production ratio, and nuclide concentrations were not consistent with surface exposure, when the samples were buried. This result does in fact suggest an outwash origin for these sediments: the alternative, Missouri River alluvium, would be expected to contain both outwash and western-derived nonglacial river sediment, and have nuclide concentrations such as we observed in sand from the nearby Platte River (sample 02-TILL-005-PLA; figs. 3, 6).

Nuclide concentrations near and below steady-state values.—After very long burial times ($\sim$ 5 x 10^6 yr), the concentration of nuclide j in a sample buried at depth z will asymptotically approach a steady state $N_{j,ss}$ where nuclide production and decay are balanced, that is, $P_j(z) = N_{j,ss}\lambda_j$ (see figs. 2C-2E). Many of the surface and subsurface samples we analyzed had nuclide concentrations that are close to steady-state values at burial depths of 4000 to 8000 g cm^{-2} (compare fig. 5 with figs. 2C-2E). If these samples had nuclide concentrations consistent with surface exposure at the time of burial, their present nuclide concentrations would imply burial ages exceeding 5 Ma, which is unlikely in light of the lack of evidence for Northern Hemisphere glaciation at that time. It is more likely that these sediments were buried with nuclide concentrations

TABLE 6

^{26}Al and ^{10}Be concentrations in pre-Wisconsinan samples of known age.

Sample name	Borehole	Depth (m)	[^{10}Be] (10^4 atoms g^{-1})	[^{26}Al] (10^4 atoms g^{-1})	Description
5-A-75-167*	5-A-75	50.9	7.84 ± 0.20	23.1 ± 1.1	Paleosol
17-A-76-146*	17-A-76	44.5	14.80 ± 0.37	40.3 ± 2.0	Paleosol
4-A-75-107	4-A-75	32.6	18.02 ± 0.54	65.7 ± 2.3	Sand and silt
1-A-76-204	1-A-76	62.2	25.27 ± 0.67	58.6 ± 3.4	Sand and silt
02-TILL-000-KRA	n/a	n/a	9.12 ± 0.38	30.0 ± 1.7	Sand and gravel 1.5 m above Lava Creek ash
02-TILL-002-KRA	n/a	n/a	5.05 ± 0.24	18.4 ± 1.3	Sand and gravel immediately below ash
02-TILL-003-KRA	n/a	n/a	4.41 ± 0.24	15.6 ± 1.9	Sand and gravel 15 cm below ash
02-TILL-004-KRA	n/a	n/a	6.31 ± 0.31	15.0 ± 1.0	Sand and gravel 30 cm below ash

*Mean of two analyses

near steady-state at their eventual burial depth, that is, with $^{26}Al/^{10}Be$ ratios well below the production ratio. Furthermore, near-steady-state concentrations make it nearly impossible to calculate accurate burial ages even if initial nuclide concentrations at the time of burial are known exactly, for two reasons. First, the closer the initial concentrations are to the steady-state values, the less time resolution is available. Second, the calculated burial age becomes very sensitive to the choice of model for nuclide production by muons.

We also found that some samples had nuclide concentrations that were below the steady-state nuclide concentrations expected at their burial depth. These occurred in the upper parts of UMRB-1 and UMRB-3. This inconsistency reflects either erosion at these sites or redeposition of material that was previously more deeply buried. Patterson (1999) inferred from stratigraphic evidence that the Des Moines Lobe had removed pre-existing older tills in this region; thus we favor erosion as an explanation for these data.

Summary: We Can Not Determine the Burial Age of Pre-Wisconsinan Fluvial Sediment from ^{26}Al and ^{10}Be Measurements.

We conclude that fluvial and glaciofluvial sands intercalated with pre-Wisconsinan tills, like modern river sands in Minnesota, were deposited and buried with initial nuclide concentrations that were not consistent with surface exposure. Therefore, we cannot use the simple burial dating methods described in the *$^{26}Al/^{10}Be$ Dating of Buried Sediments in Simple Situations* section, which rely on assuming that initial nuclide concentrations were consistent with surface exposure, to date the tills.

Limiting Ages Derived from Conservative Assumptions

Even though we cannot determine the exact burial age for most samples of pre-Wisconsinan sand, we can compute maximum and minimum limiting ages for some parts of the stratigraphy by making conservative assumptions.

First, given a sample buried by some thickness of overburden, we can estimate its minimum possible burial age, that is, the minimum age of the lowest unit in the overburden, by making the following assumptions:

1. The $^{26}Al/^{10}Be$ ratio of the sample at the time of burial was 4.3 ($R^*_{26/10} = 0.7$ for comparison with figures), the average of our analyses of Wisconsinan glacial sediment from the Minnesota River Valley. We justify this value as the minimum $^{26}Al/^{10}Be$ ratio that any Pleistocene fluvial sediment could reasonably be expected to have had by the observation that nuclide concentrations in modern fluvial sediments directly reflect those in Wisconsinan glacial sediments, which are near the average $^{26}Al/^{10}Be$ ratio observed for all our analyses of the entire Pleistocene section. If each ice sheet advance remobilizes a representative sample of the sedimentary section that exists at that time, the $^{26}Al/^{10}Be$ ratio of fluvial sediments at burial should decrease with each glaciation. Although this decrease in $^{26}Al/^{10}Be$ ratio is not strictly assured, only very complicated scenarios can produce lower fluvial $^{26}Al/^{10}Be$ ratios at burial in pre-Wisconsinan river sands than in modern river sands. Our estimates of the $^{26}Al/^{10}Be$ ratio at burial for pre-Wisconsinan sands, discussed above, are all greater than 4.3.
2. The sample was immediately buried at infinite depth and remained so until the present time, that is, $P_j(z) = 0$ always. This procedure ensures an underestimate of the true burial age.

With these assumptions, the minimum burial age for the sample is:

$$t_{\min} = \frac{-\ln\left(\frac{R}{4.3}\right)}{\lambda_{26} - \lambda_{10}} \tag{11}$$

where R is the measured $^{26}Al/^{10}Be$ ratio. We cannot calculate a meaningful minimum age with these assumptions for samples whose nuclide concentrations are not clearly distinguishable from those of modern fluvial sediments (as is the case for all samples in borehole UMRB-2, and several others). This calculation yields the minimum age for the sample, which by the principle of superposition also applies to any unit that is stratigraphically below the sample. Likewise, for boreholes with multiple samples at different stratigraphic levels, minimum ages calculated for samples at higher stratigraphic levels also apply to underlying units. Figure 8 summarizes these results. We have not considered analytical uncertainty in calculating these minimum ages.

Estimating the maximum burial age associated with a sample is more complicated, because of the fact that, until the sample is buried deeply enough that the nuclide concentration in the sample lies above the steady-state nuclide concentration at that depth, infinitely long cyclical burial histories are permitted. Thus, we cannot associate a maximum age with a particular unit that we have sampled, but we can use a particular sample to provide maximum ages for stratigraphic units that lie above it by some critical amount. In effect assignment of maximum ages is done by assuming that, at the time of emplacement of the overlying unit of interest, the sample had nuclide concentrations in equilibrium with surface exposure, and since that time the sample has been buried at the minimum possible depth allowed by the stratigraphy. We provide a mathematical justification in the Appendix.

Figure 8 shows the results of these calculations, which provide slightly more information on the age of the tills than was previously available. The age of intermediate-depth tills in borehole UMRB-1 [unit 8 of Patterson (1999) and adjacent tills] is constrained to be between ca. 0.6 and ca. 1.5 Ma. The oldest tills in the Prairie Coteau section (boreholes SWRA-3 and SD-BR) must be older than 1 to 1.25 Ma; the youngest tills in this section are younger than 1.5 Ma. These data are little help in correlating individual tills on the basis of age, but do indicate that nearly all of the pre-Wisconsinan tills are older than previously believed.

Explicit Burial Ages for One Special Case

We collected two samples from the basal sand unit in borehole SD-CO (samples SD-CO-402 and -406; fig. 9; table 2). This unit directly overlies saprolite, and it and similar sands in other boreholes underlie all known tills in the region. If it predated all ice sheet advances, the fact that modern river sands in unglaciated regions have ^{26}Al and ^{10}Be concentrations that comply with equation (5) suggests that this unit would, at burial, have had nuclide concentrations consistent with surface exposure as well. In addition, this unit has extremely high concentrations of atmospherically produced ^{10}Be (Balco, ms, 2004b), which further suggests that it originated from a preglacial landscape and reflects a long period of surface exposure. Thus, the available evidence indicates that these samples were buried with nuclide concentrations in equilibrium with surface exposure, and we can use them to determine the age of the overlying till by the simple burial dating approach described in the *$^{26}Al/^{10}Be$ Dating of Buried Sediments in Simple Situations* section. The major remaining uncertainty in this calculation concerns the burial history of this sample after the emplacement of the lowest till unit. If we calculate the burial age under the assumption that only the lowest till was emplaced at the time of interest, and the rest of the section was emplaced recently, we will overestimate the true burial age; likewise, if we assume that the entire present overburden was emplaced at once we will underestimate the true age. Neither of these

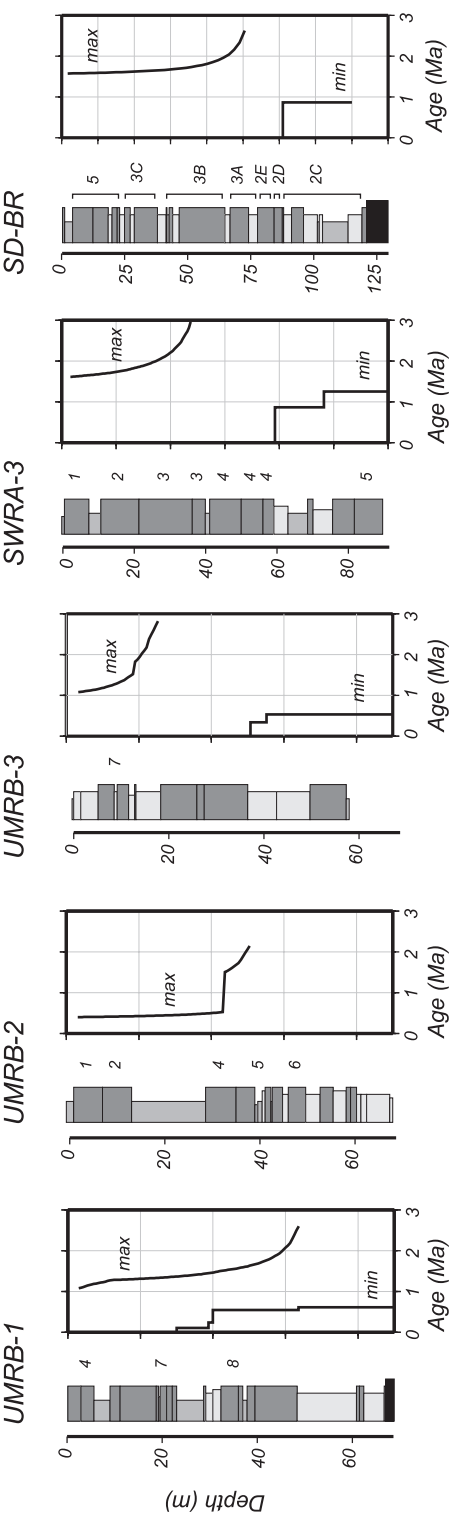

Fig. 8. Minimum and maximum limiting age constraints inferred from ^{26}Al and ^{10}Be measurements for boreholes that contained pre-Wisconsinan sand samples, calculated as described in the *Limiting Ages Derived from Conservative Assumptions* section and Appendix. Lithologic symbols are the same as those in figure 5. Numbers for till units in boreholes UMRB-1, -2, and -3 follow Patterson (1999), those in SWRA-3 follow Patterson (1997), and those in SD-BR follow Lineburg (1993).

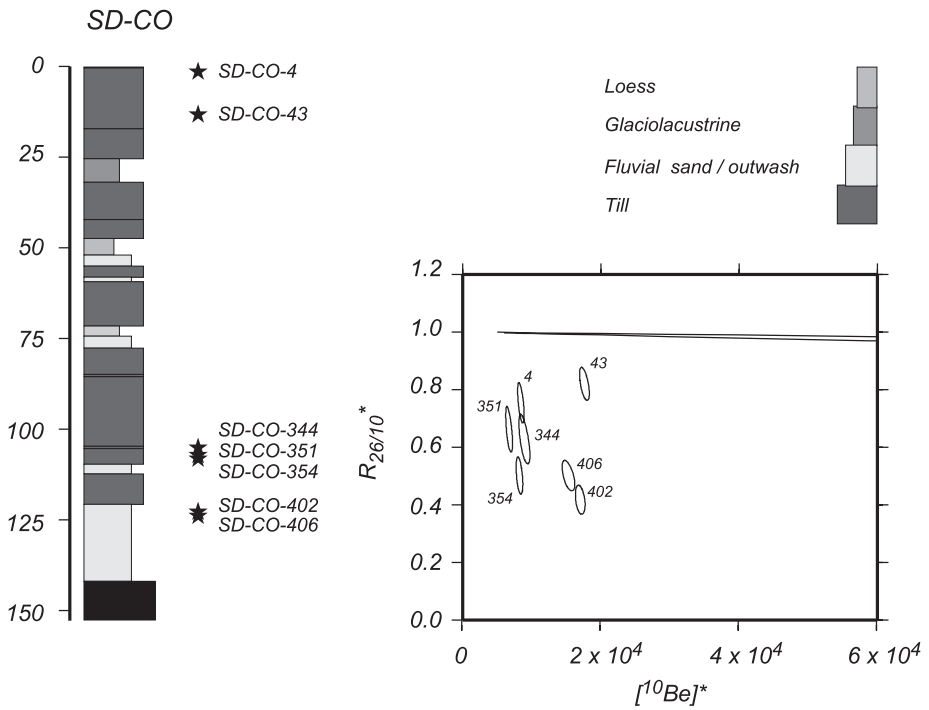

Fig. 9. Stratigraphy and analytical data for borehole SD-CO. Left panel, borehole stratigraphy. Stars and accompanying sample names denote sample locations in borehole. Right panel, ^{26}Al and ^{10}Be concentrations.

end-member scenarios is likely to be true, so we used the following assumptions, which we believe to be the most reasonable:

1. Nuclide concentrations at the time of burial by the lowest till reflect equilibrium with steady erosion, that is, equation (5) applies. In applying equation (5), we use approximate regional average surface production rates of 7.5 and 45.8 atoms g^{-1} yr^{-1} for ^{10}Be and ^{26}Al respectively. Note that the choice of surface production rates here does not affect the burial age, only the erosion rate in the sediment source area ϵ that we might also infer from the samples.
2. There have been four subsequent periods of burial, that is, K=4 in equation (9), as follows: First, the samples were buried at 2500 g cm^{-2} depth at an unknown time by the till immediately overlying them. Second, they were buried at 10,100 g cm^{-2} depth, by the till whose top is now 77 m below the surface, at 1 Ma. This age estimate is based on the analysis of the truncated paleosol that we discuss below in the *Example Paleosol in Eastern South Dakota* section. Third, they were buried to 23,500 g cm^{-2} depth, by the sequence of tills whose top is now 17 m below the surface, at 0.5 Ma. This age estimate is speculative but, as the samples are already very deeply buried at this point, has a minimal effect on the actual burial age. Fourth, they were buried to their present depth of 27,200 g cm^{-2} by the uppermost, late Wisconsinan, till 30,000 yr ago.
3. We disregard the fact that the site was covered by thick ice during past glaciations, which is important because several hundred meters of ice cover would essentially stop nuclide production entirely. By analogy to the most

recent glacial-interglacial cycle, the site might have been covered by thick ice for up to 25 percent of its entire history. However, the fact that the lowest till is relatively thick, so nuclide production rates after burial are very low under any circumstances, means that the possibility of occasional subsequent ice cover is less important than either the other large uncertainties in the burial history, or the analytical uncertainties. It would become important to account for periods of ice cover if our analyses were more accurate, or if we had more information about the age of the overburden.

Thus, in the framework of equation (9), $z_{i,1} = 2500$ g cm^{-2}, $z_{i,2} = 10{,}100$ g cm^{-2}, $z_{i,3} = 23{,}500$ g cm^{-2}, $z_{i,4} = 27{,}200$ g cm^{-2}, $t_2 = 0.5 \times 10^6$ yr, $t_3 = 0.47 \times 10^6$ yr, and $t_1 = 30{,}000$ yr. t_1 is the unknown parameter of interest, and t_4 is the age of the till overlying the samples.

With these assumptions we can determine t_1 and the nominal erosion rate prior to burial ϵ by using equations (5) and (9) to predict the expected nuclide concentrations as a function of these unknown parameters, and then finding ϵ and t_1 that best explain the measured nuclide concentrations. We are not interested in ϵ so we treat it as a nuisance parameter. For sample SD-CO-402, this calculation yields ages for the lowermost till of 1.90 ± 0.24 Ma and 2.03 ± 0.30 Ma, using the muon interaction cross-sections from the Wyangla Quarry profile and from Heisinger and others (2002a, 2002b), respectively. Sample SD-CO-406 yields ages of 1.43 ± 0.18 Ma and 1.50 ± 0.22 Ma, respectively. These standard errors include only analytical uncertainty.

These age estimates are surprisingly young, because the existence of tills in Nebraska and Iowa that underlie the 2 Ma Huckleberry Ridge ash (Boellstorff, 1978c; Roy and others, 2004) suggests that the oldest tills in eastern South Dakota should also be older than 2 Ma. Our analysis of SD-CO-402 is consistent with this idea; that of SD-CO-406 is not. If the disagreement between the two samples were the result of analytical error, the true age of the lowest till in SD-CO would be near 1.7 Ma; if our assumption that the nuclide concentrations in these samples were consistent with surface exposure were incorrect for SD-CO-402, this sample would overestimate the age of the till, and the true age would be near 1.5 Ma. In any case, we were not able to find any plausible burial history that would be consistent with both the data for SD-CO-406 and an age greater than 2 Ma for the till. Thus, we cannot associate the lowermost till here with pre-2 Ma tills further to the south.

Results and Discussion II: Pre-Wisconsinan Paleosols

We show in the previous section that fluvial and glaciofluvial sands intercalated with glacial tills are not suitable for burial dating using ^{26}Al and ^{10}Be. We were more successful applying the technique to paleosols developed on till and buried by younger sediments. Paleosols are common in Plio-Pleistocene glacial sediment sections, especially in the southern part of our field area. Starting with the first explorations of the north-central U.S., glacial geologists took particular note of prominent paleosols as a possible means of correlating major glacial-interglacial cycles: thus, there exist numerous well-described sections where paleosols are buried by younger glacial sediment.

There are two particular advantages to using paleosols rather than fluvial sediments from our perspective. First, the existence of a well-developed paleosol implies a long period of surface exposure. In contrast to river sands, which appear to experience very short periods of surface exposure between exhumation from old glacial deposits and transport out of the glaciated area, we expect quartz in paleosols to have higher ^{26}Al and ^{10}Be concentrations. This advantage makes for more precise analyses and also suggests that, whatever the inherited nuclide concentrations in the parent material on which the soil is developed, nuclide concentrations may return to values within the simple exposure island if the soil surface is exposed for long enough.

TABLE 7

Location of surface soil samples. Production rates calculated according to Stone (2000).

Sample name	Latitude	Longitude	elevation (m)	Nuclide production rates at surface in quartz (atoms g^{-1} yr^{-1}) ^{10}Be	^{26}Al	Description
MN-SAL	44.5575 N	93.8749 W	277	6.4	39.2	Road cut, Salisbury, MN
02-TILL-006-GRA	44.0516 N	96.2852 W	558	8.2	49.8	Soil pit, Grange, MN
02-TILL-007-PIT	44.0980 N	96.3380 W	527	8.0	48.5	Excavation, Grange, MN

Second, samples from different depths in a paleosol share a similar exposure history. This advantage enables us to collect more samples and obtain a tractable problem in which the number of measurements exceeds the number of unknown parameters [see, for example, Granger and Smith (2000) and Wolkowinsky and Granger (2004)]. In contrast, there is no assurance that sediment from different stratigraphic levels in a single fluvial sand unit will have a similar provenance and exposure history.

Examples from Modern Soils

We began by measuring nuclide concentrations in modern surface soils to determine whether or not they were consistent with surface exposure. Figure 3 and table 7 show the locations of these samples. Figure 10 and table 8 show nuclide concentrations. As expected, nuclide concentrations in quartz near the soil surface were higher, and closer to the simple exposure island, than nuclide concentrations in

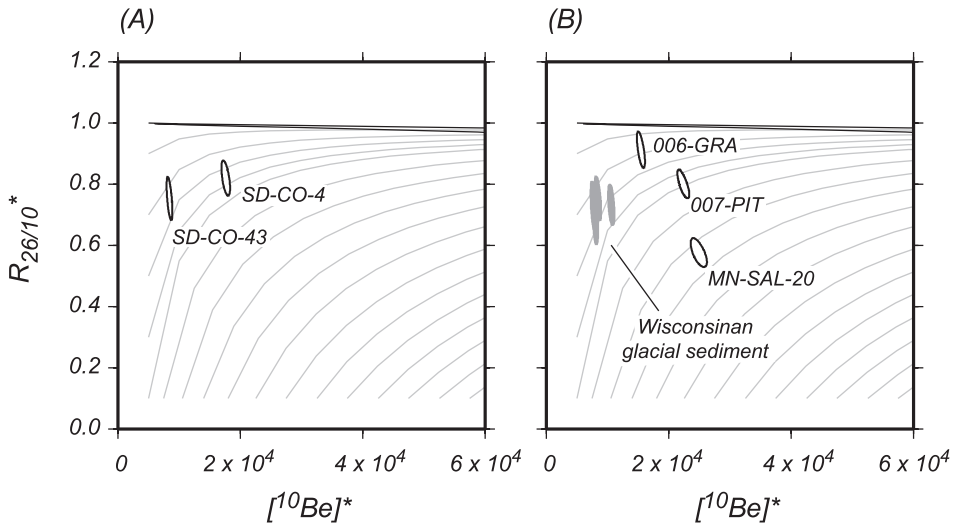

Fig. 10. Nuclide concentrations in quartz from modern surface soils in southwest Minnesota and adjacent South Dakota. (A) Nuclide concentrations in a near-surface sample (SD-CO-4) and a sample from 13 m depth (SD-CO-43) in the uppermost (Wisconsinan) till from borehole SD-CO in eastern South Dakota. The excess ^{26}Al and ^{10}Be in the surface sample are the result of exposure since deposition of the till. Light lines in background are resetting curves from fig. 2F. (B) ^{26}Al and ^{10}Be concentrations in quartz from soils in southwest Minnesota. Light lines in background are resetting curves from fig. 2F. Gray ellipses show ^{26}Al and ^{10}Be concentrations in nearby Wisconsinan glacial sediments from figure 6.

TABLE 8

^{26}Al and ^{10}Be concentrations in surface soil samples.

Sample name	[^{10}Be] (10^4 atoms g^{-1})	[^{26}Al] (10^4 atoms g^{-1})	Description
MN-SAL-20	15.95 ± 0.57	56.2 ± 2.4	Upper 20 cm of soil on Wisconsinan till
02-TILL-006-GRA	12.60 ± 0.36	70.1 ± 2.3	Surface sample of soil on pre-Wisconsinan till
02-TILL-007-PIT	17.85 ± 0.53	86.9 ± 2.3	Surface sample of soil on Wisconsinan outwash
SD-CO-4	14.36 ± 0.40	72.0 ± 2.9	Soil on Wisconsinan till at 1.3 m depth in borehole SD-CO

quartz from the soil parent material, that is, Wisconsinan glacial sediment, well below the surface.

In borehole SD-CO, we analyzed samples from a soil developed on the uppermost (Wisconsinan) till, which is associated with the Verdi ice-marginal position of the Des Moines lobe and was deposited ca. 30,000 ^{14}C yr B.P. (Setterholm, 1995; Patterson, 1997). A sample at 13 m depth (SD-CO-43), which reflects only the inherited nuclide concentration in the till when it was emplaced, had low nuclide concentrations that were inconsistent with surface exposure, like other samples of Wisconsinan glacial sediment (compare figs. 10A and 6). A sample from 1.2 m depth in the same borehole (SD-CO-4) had higher nuclide concentrations that lay along an appropriate resetting curve relative to the lower sample (figs. 10A and 9). Differencing the two samples yields exposure ages of 43,000 ± 5000 yr and 38,000 ± 4000 yr for the ^{10}Be and ^{26}Al measurements respectively. These ages are somewhat older than the age of the till inferred from correlation to the Verdi ice margin, but the difference in ages can be accounted for by our uncertainty in determining the exact depth of sample SD-CO-4 prior to disturbance of the drilling site.

We also sampled the uppermost part of the modern soil at three other locations (fig. 10; tables 7, 8; locations in fig. 3). We collected sample 02-TILL-007-PIT from the surface of a soil developed on Wisconsinan outwash associated with the Bemis ice-marginal position (14,000 ^{14}C yr B.P.; Setterholm, 1995; Patterson, 1997). We did not measure nuclide concentrations at depth here; however, if they were similar to those in other latest Wisconsinan deposits of the Des Moines lobe that we sampled, this sample would reflect 15,000 years of exposure, which is consistent with the age of the unit. We collected sample 02-TILL-006-GRA from what we believed to be an undisturbed soil surface developed on pre-Wisconsinan till (Setterholm, 1995; Patterson, 1997). This sample had surprisingly low nuclide concentrations, equivalent to 10,000 to 15,000 yr of surface exposure if the parent material had nuclide concentrations similar to late Wisconsinan tills. It is difficult to explain these concentrations unless much of the quartz in the surface soil originated from late-glacial or Holocene eolian deposition, and not from the older till on which the soil is developed. Finally, we collected sample MN-SAL-20 from the upper 20 cm of a soil developed on Wisconsinan till deposited 12,000 to 14,000 ^{14}C yr B.P. The difference between the ^{10}Be concentration in this sample and that in Wisconsinan glacial sediments elsewhere indicates 15,000 years of exposure. The ^{26}Al concentration in this sample was surprisingly low (suggesting only 8000 yr of exposure with equivalent assumptions); this low concentration of ^{26}Al suggests that the inherited nuclide concentrations in the till at this site were somewhat lower than in the other Wisconsinan glacial sediment we sampled.

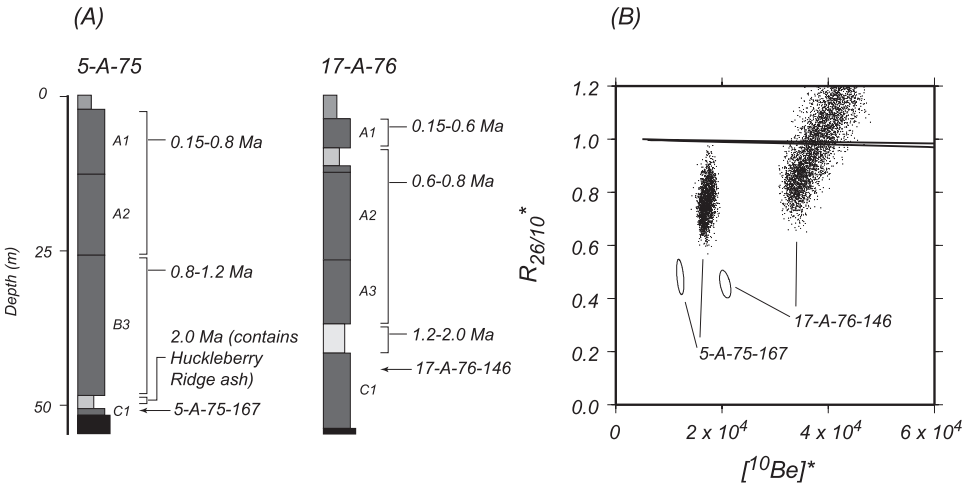

Fig. 11. (A) Stratigraphy of boreholes 5-A-75 and 17-A-76, showing age constraints for units overlying our samples (Boellstorff, 1978a). (B) Measured nuclide concentrations in samples (68% confidence ellipses) and possible nuclide concentrations at the time of burial (dots) generated from Monte Carlo simulation described in text. Inferred nuclide concentrations at the time of burial that have $R^*_{26/10} > 1$ indicate that the corresponding burial histories cannot be correct even though they fit the independent age constraints; however, we have retained them to show that the probability distribution is centered on the simple exposure island.

Direct Measurements on Buried Paleosols of Known Age

Our measurements from modern soils show, as we expect from figure 2F and the nuclide concentrations we measured in Wisconsinan glacial sediments (fig. 6), that the present interglaciation has been too short to "reset" nuclide concentrations in modern soils to the simple exposure island. However, many paleosols found intercalated with early and middle Wisconsinan tills display soil development that suggests much longer periods of surface exposure. In these cases the assumption, that nuclide concentrations in these soils were consistent with surface exposure when buried by overlying tills, would be more plausible.

We evaluated this assumption by analyzing samples from two paleosols of approximately known age in drillcores from southeast Iowa collected by Boellstorff (1978a) (fig. 11; table 6). Both paleosols are developed on the "C1" till of Boellstorff (1978a, 1978b, 1978c), which is equivalent to the upper of the two "R2" tills of Roy and others (2004). This till is magnetically reversed and underlies the 2.0 Ma Huckleberry Ridge ash. We used a Monte Carlo simulation similar to the one we describe above in the *$^{26}Al/^{10}Be$ Ratios Below the Production Ratio in River Sands From Prior Interglacials?* section to generate random burial histories that fit the existing age constraints, and thus compute the initial nuclide concentrations that the samples could have had when they were buried.

In borehole 5-A-75 (Boellstorff, 1978b), our sample is overlain by silt containing the Huckleberry Ridge ash, which we assumed was deposited 2.0 Ma, then by a magnetically reversed till ("B" or "R1" till) deposited 1.2 to 0.78 Ma, and then by two magnetically normal tills ("A1" and "A2" or "N") deposited 0.78 to 0.15 Ma. Only very few burial histories that fit these constraints result in nuclide concentrations at burial that are consistent with surface exposure (fig. 11).

In borehole 17-A-76, our sample is overlain by silt which is most likely correlative with sand and silt in nearby boreholes that was deposited 2 to 1.2 Ma, then by two tills ("A2" and "A3") deposited 0.78 to 0.62 Ma, then by a third till ("A1") deposited 0.62 to

0.15 Ma. Many plausible burial histories that fit these constraints yield initial nuclide concentrations close to the simple exposure island (fig. 11), suggesting that the sample most likely had nuclide concentrations at burial that were consistent with surface exposure. The difference in our results for these two samples is consistent with the relative degree of development of the two paleosols (J. Mason, unpublished core logs) as well as the higher overall ^{10}Be and ^{26}Al concentrations in 17-A-76-146 than in 5-A-75-167.

General Method for Calculating Burial Ages for Paleosols

We conclude from these measurements that pre-Wisconsinan paleosols that were formed during particularly long interglaciations may or may not contain quartz with nuclide concentrations consistent with surface exposure. Thus, we cannot in general use simplifying assumptions to estimate the ^{26}Al and ^{10}Be concentrations in soil quartz at the time of burial, but must treat them as unknown parameters. Although this ambiguity presents a fatal difficulty for interpreting buried fluvial sediments, it does not present the same difficulty for paleosols. A paleosol developed on a well-mixed parent material such as till contains quartz grains that, on average, were emplaced with the same initial nuclide concentrations. The additional nuclide inventory produced by exposure during soil formation will vary throughout the soil profile as a known function of depth. The entire paleosol has the same exposure and burial history. These facts mean that we can determine the burial age of a paleosol using an exposure model with only four unknown parameters: initial ^{10}Be and ^{26}Al concentrations at the time of till emplacement, the duration of soil formation, and the duration of burial. In contrast to the case for fluvial sediment, where we could not simultaneously determine all of these parameters because none of them were shared between different samples, we can collect multiple samples from various depths in a paleosol to obtain a tractable problem in which the number of measurements greatly exceeds the number of unknowns. The mathematical procedure for calculating the parameter is the same as we have described above: we use equation (9) to predict the measured nuclide concentrations for given parameters, then use an optimization method to determine the parameters which best reproduce the observations. We describe this method in more detail in Balco and others (2005).

Example Paleosol from Eastern Nebraska

We give two examples of how to apply this approach to buried paleosols: first, in an ideal situation where a well-developed paleosol is entirely preserved, and second, in a more difficult situation where the paleosol is not only weakly developed, but the upper part of the soil profile was also truncated by the emplacement of a later till. In the first example, we measured ^{26}Al and ^{10}Be concentrations at six depths below the surface of a paleosol developed on the youngest till in eastern Nebraska and buried by three loess units. We have previously reported these data in Balco and others (2005). Figure 12 and table 9 show the stratigraphy of this borehole and the nuclide concentrations in the paleosol. Here the initial nuclide concentrations at the time of emplacement of the till $N_{i,0}$ are unknown parameters that are the same for all samples. The upper two loess units, the Peoria and Loveland formations, were deposited 12,000 to 35,000 and 135,000 to 150,000 yr ago, respectively (Forman and others, 1992; Forman and Pierson, 2002). Thus, $K = 4$, $t_3 = 135{,}000$ yr, and $t_4 = 35{,}000$ yr. t_2, the time between emplacement of the first and second loess units, is unknown, and the age of the lowermost loess, that is, $t_2 + t_3 + t_4$, is the unknown parameter of most interest. t_1, the nominal duration of soil formation, cannot be determined exactly without knowing the erosion rate during soil formation, and we treat it as a nuisance parameter (see further discussion in Balco and others, 2005). The burial depths for the various time periods are $Z_2 = 1600$ g cm^{-2}, $Z_3 = 3100$ g cm^{-2}, and $Z_4 = 5100$ g cm^{-2}.

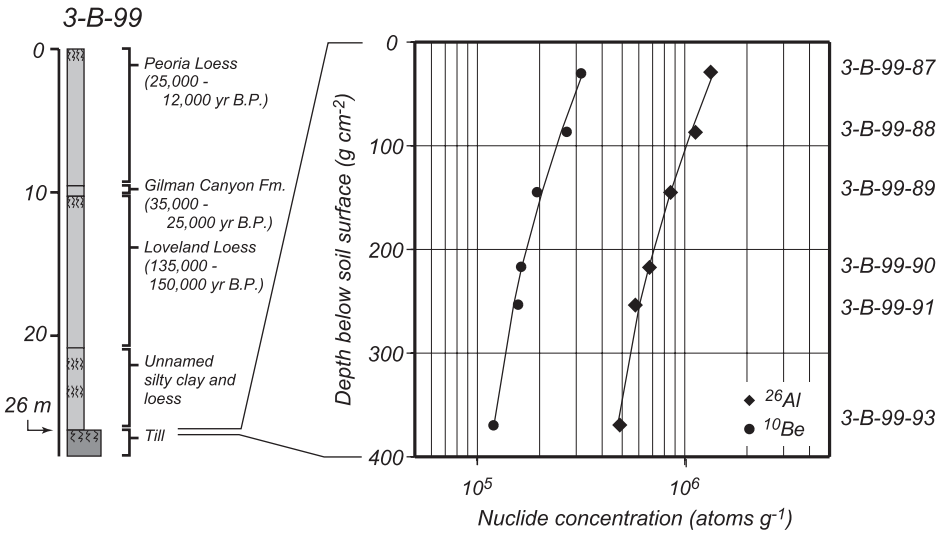

Fig. 12. Left panel, stratigraphy of borehole 3-B-99 from eastern Nebraska. Right panel, ^{26}Al and ^{10}Be concentrations in quartz samples from paleosol at 26 m depth in borehole. Analytical errors are smaller than the symbols used to plot the data at this scale. Lines show nuclide concentrations predicted by best-fit burial history described in the text. These data are also reported in Balco and others (2005).

To summarize, the unknown parameters in this problem are the initial nuclide concentrations $N_{j,0}$ and the durations of exposure and initial burial, t_1 and t_2. The values of these parameters that best fit the data are as follows: $N_{10,0} = 0.78 \times 10^5$ atoms g^{-1}; $N_{26,0} = 2.6 \times 10^5$ atoms g^{-1}; $t_1 = 53{,}000$ yr; and $t_2 = 420{,}000$ yr., that is, the most likely age of the lowermost loess is 0.57 Ma.

We estimated the uncertainty in this age determination with a Monte Carlo simulation in which we repeatedly generated random sets of measurements drawn from normal probability distributions with mean and standard deviation given by our actual measurements and their analytical uncertainties. We then found the age that best fit each simulated data set. This exercise indicates that the lowermost loess was deposited 0.57 ± 0.12 Ma. Figure 13 shows the results of this simulation. The analytical

TABLE 9

Sample depths and nuclide concentrations, paleosol at 26 m in borehole 3-B-99. These data also appear in Balco and others (2005).

Sample name	Depth in borehole (m)	Depth below soil surface (g cm^{-2})	[^{10}Be] (10^4 atoms g^{-1})	[^{26}Al] (10^4 atoms g^{-1})
3-B-99-87	26.01-26.31	0-58	31.9 ±1.1	133.8 ± 4.3
3-B-99-88	26.31-26.62	58-117	26.83 ± 0.93	112.7 ± 3.3
3-B-99-89	26.62-26.92	117-175	19.75 ± 0.58	85.6 ± 3.8
3-B-99-90	27.07-27.23	204-234	16.14 ± 0.49	67.6 ± 3.5
3-B-99-91	27.32-27.46	234-278	15.75 ± 0.47	57.9 ± 2.1
3-B-99-93*	27.76-28.14	336-410	11.92 ± 0.28	48.7 ± 1.9

*Mean of two analyses

*Mean of two analyses

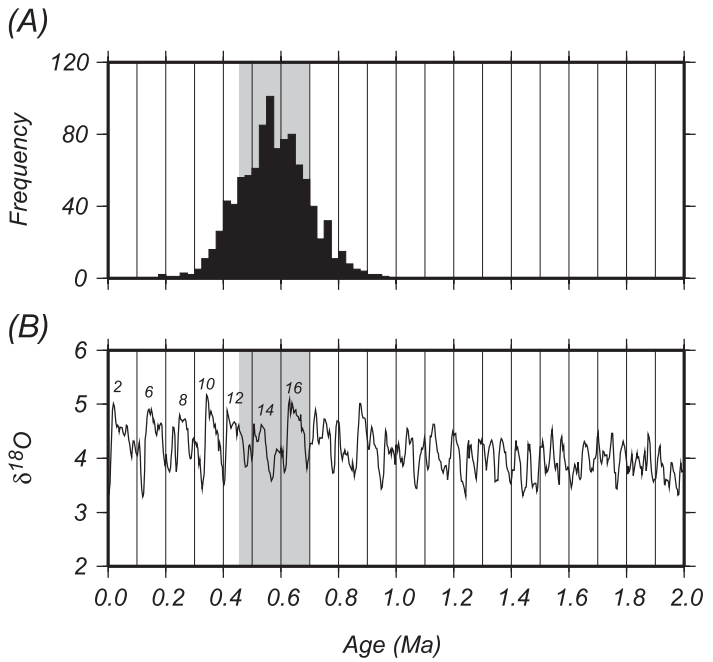

Fig. 13. Error analysis for the age of the lowermost loess unit in borehole 3-B-99. (A) Probability distribution of best-fit ages generated by the Monte Carlo simulation described in the text. The gray band shows ± 1 σ uncertainty range. (B) Benthic $\delta^{18}O$ record from Shackleton (1995). These data are also published in Balco and others (2005).

error in our measurements of ^{26}Al concentrations is the dominant source of uncertainty. The uncertainty in muon interaction cross-sections is unimportant in this particular case because of the relatively high ^{26}Al and ^{10}Be concentrations in the paleosol and the relatively short duration of burial: reduction of the preexisting nuclide inventory by decay is much more important than nuclide production during burial. We conclude that the loess was emplaced during marine $\delta^{18}O$ stages 13 to 15. We cannot accurately determine the duration of soil formation, and thence the age of the underlying till, because we lack information about the surface erosion rate during soil development; however, it is most likely that this till was emplaced during marine $\delta^{18}O$ stage 16 near 0.62 Ma. The $N_{j,0}$, the initial nuclide concentrations in the till at the time of emplacement, are similar to those we observed in Wisconsinan tills.

Example Paleosol in Eastern South Dakota

In the second example, we applied the same method to the oxidized upper portion of a till at 103.8 m depth in borehole SD-CO from eastern South Dakota (table 10; figs. 9, 14).

This example presented several difficulties compared to the soil in core 3-B-99 described above. First, in contrast to the complete, well-developed soil profile in 3-B-99, oxidation and a weakly developed blocky structure are the only indications of soil development. Nuclide concentrations near the surface of this till (with the exception of one anomalous ^{10}Be measurement which we discuss below) decrease exponentially with the appropriate attenuation length (fig. 14), which confirms that exposure within several meters of the surface, did in fact take place. However, the upper part of the soil profile is not preserved. This indeterminate amount of truncation of the soil profile makes it impossible to determine the exposure time of the soil

TABLE 10

Sample depths and nuclide concentrations, paleosol at 104.7 m depth in borehole SD-CO.

Sample name	Depth in borehole (m)	Depth below till surface $z_{i,0}$ (g cm^{-2})	[^{10}Be] (10^4 atoms g^{-1})	[^{26}Al] (10^4 atoms g^{-1})
SD-CO-344	104.7-105.0	0-58	7.28 ± 0.44	27.8 ± 2.0
SD-CO-351	107.0-107.3	434-492	5.48 ± 0.28	22.1 ± 0.4
SD-CO-354	107.9-108.2	608-666	6.71 ± 0.27	20.5 ± 1.6

prior to burial (because we cannot accurately estimate nuclide production rates during soil formation), but does not affect our estimate of the burial age for the soil. Thus, we again treat the duration of exposure during soil formation t_1 as a nuisance parameter. On the other hand, the fact that we have only the deepest part of the soil profile to work with indicates that we can disregard vertical mixing of quartz during soil development, which simplifies the problem.

Second, we have little information about the age of any of the overlying units. The till immediately overlying the samples, whose age is the unknown parameter of interest, is 4300 g cm^{-2} thick; at present the samples are buried by 22,300 g cm^{-2} of overburden, of which the uppermost 3800 g cm^{-2} is late Wisconsinan in age. In the framework of equation (9), $K = 2$, t_1 is the parameter of interest, and the Wisconsinan burial history is represented by t_2 = 25,000 yr, and $z_{i,2}$ = 22,300 g cm^{-2}. The uncertainty in the time at which the intermediate 14,200 g cm^{-2} of material was deposited leads to an uncertainty in the parameters $z_{i,1}$. To evaluate the importance of

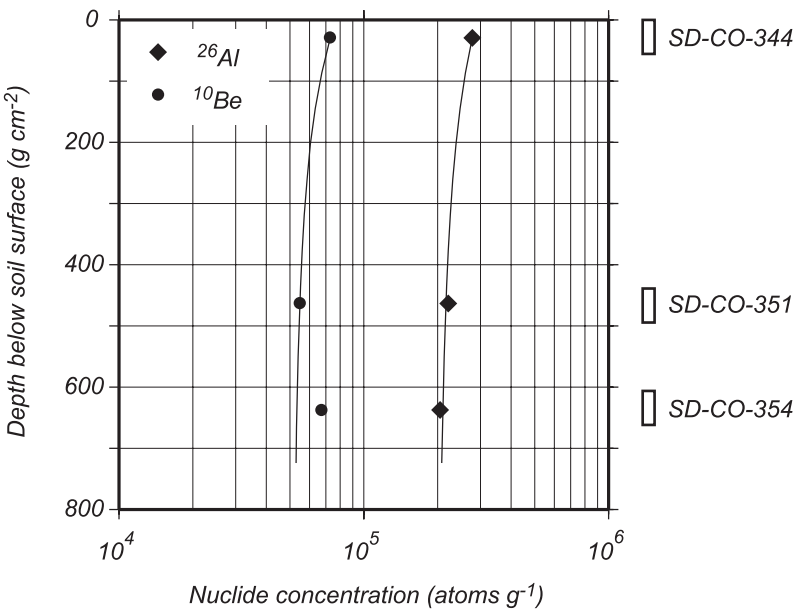

Fig. 14. ^{26}Al and ^{10}Be concentrations in quartz from the paleosol at 103.8 m depth in borehole SD-CO. Analytical errors are smaller than the symbols used to plot the data at this scale. Boxes at right show length of core that we agglomerated to obtain each quartz sample. The lines show nuclide concentrations predicted by the best-fit burial history described in the text. We excluded the ^{10}Be measurement for SD-CO-354 in computing the fit, as described in the text.

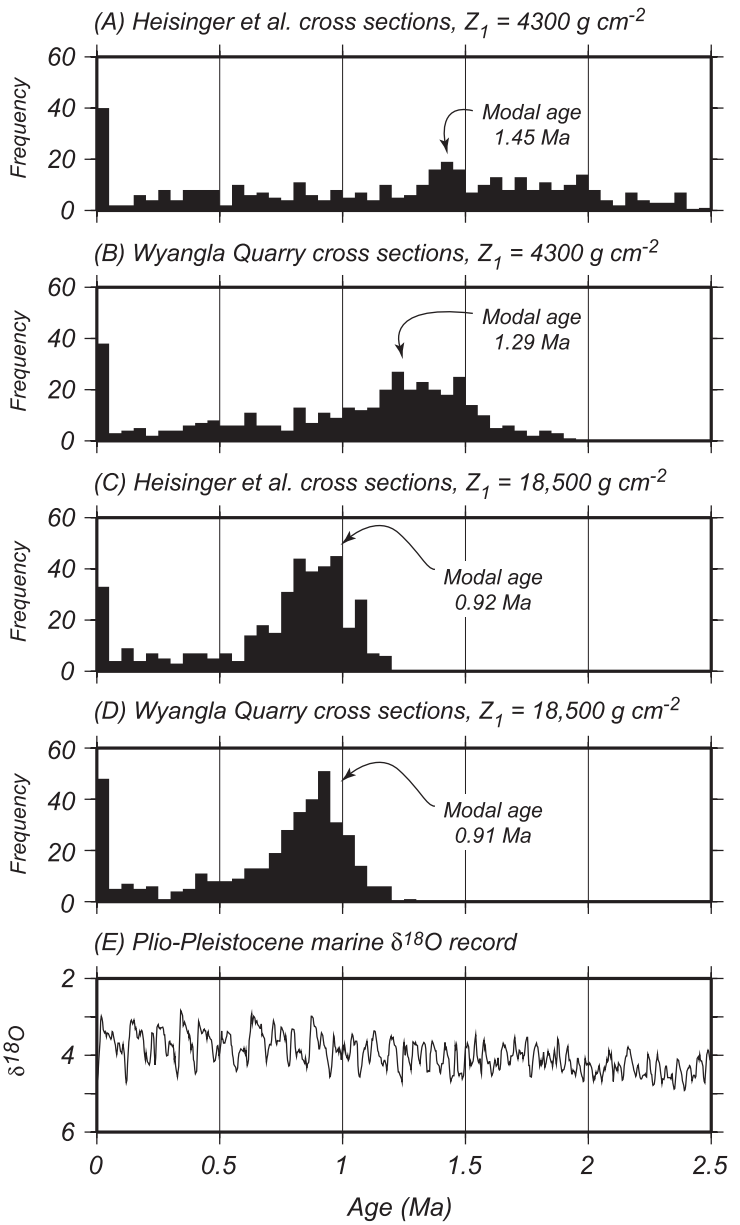

Fig. 15. Error analysis for burial age of paleosol in borehole SD-CO, part I. Histograms (A)-(D) show results of Monte Carlo error analyses for bracketing assumptions about initial burial depth and muon interaction cross-sections. Arrows indicate modal ages. (E) Shows benthic $\delta^{18}O$ record from Shackleton (1995).

this uncertainty, we carried out the calculation with the two end member scenarios of a) Z_1 = 4300 g cm^{-2}, that is, all the overburden above the till of interest was emplaced 25,000 yr ago, and b) Z_1 = 18,500 g cm^{-2}, that is, all the overburden below the Wisconsinan was emplaced at once at the time of interest. Figure 15 summarizes these results.

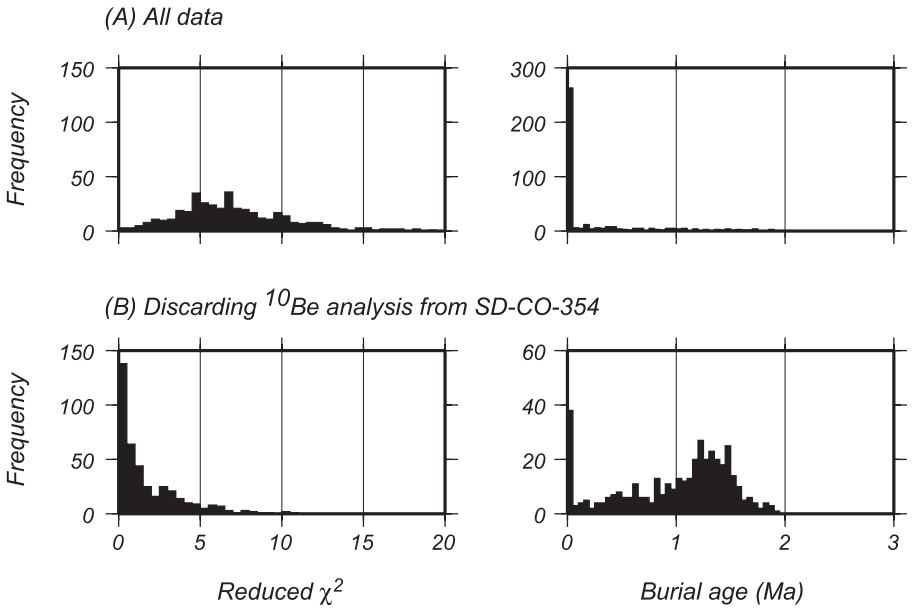

Fig. 16. Error analysis for burial age of paleosol in borehole SD-CO, part II. Histograms show probability distributions for reduced χ^2 goodness-of-fit statistic (at left) and best-fit burial ages (at right) for exposure models generated by Monte Carlo analysis. (A) All nuclide measurements included. The best-fit burial age is near zero but the fit to the data is unacceptable. (B) Omitting ^{10}Be measurement from SD-CO-354. Stratigraphically plausible burial ages near 1.3 Ma yield acceptable fits to the data. The Wyangla Quarry muon interaction cross-sections (see text) and $Z_1 = 4300$ g cm^{-2} were used in the calculation.

Third, as nuclide concentrations in the sample are much lower than in 3-B-99, nuclide production during burial, which is predominantly by muon interactions, is correspondingly more important relative to decay of the initial nuclide inventory. Thus the uncertainty in rates of nuclide production by muons is important. We evaluated its importance by carrying out the calculation with both sets of muon interaction cross-sections (fig. 15). As expected, the choice of cross-sections is most important when most of the burial takes place at shallow depths.

Fourth, the nuclide concentrations in these samples are low, and have correspondingly large analytical uncertainties. Furthermore, nuclide concentrations are close to steady-state values for depths of 8000 to 12,000 g cm^{-2}, which causes analytical errors in nuclide concentration to propagate into large errors in age. In addition, it means that implausible burial histories, in which the initial nuclide concentrations $N_{i,0}$ are very close to the measured concentrations, and the exposure and burial times t_1 and t_2 are both zero, fit the full data set better than stratigraphically plausible burial histories with t_1 on the order of 4) yr and t_2 on the order of 6) yr. However, neither of these scenarios fit the data acceptably well. This problem is evident in the error analysis (which we carried out using a Monte Carlo simulation as described above) by the large population of possible results with burial age equal to zero, and the uniformly poor fit of the model to the data (reduced $\chi^2 = 5 \pm 3$; fig. 16). We found that this difficulty in fitting the data was largely explained by a single analysis, our ^{10}Be measurement for the lowest sample (SD-CO-354). When we did not consider this measurement in determining the best-fit burial history, the plausible burial histories fit the data well (reduced $\chi^2 \sim 1$; fig. 16). As an anomalously high ^{10}Be concentration is consistent with the possibility of under correction for spurious ^{10}Be in the cathodes used for AMS analysis

(discussed above in ANALYTICAL METHODS section), we discarded this analysis. Regardless, the relatively large analytical uncertainties, and the proximity of measured nuclide concentrations to steady-state concentrations, result in a larger uncertainty in our age estimate for this paleosol than for the one in borehole 3-B-99.

Figure 15 summarizes the results of the error analysis for bracketing assumptions about muon cross-sections and burial history. With assumptions that minimize nuclide production rates after burial, the age of the till overlying this paleosol is fairly well constrained to be near 0.9 Ma. For the opposite assumptions, the probability distribution of the age of the till is very wide, with a modal age near 1.45 Ma. As the most likely burial history is intermediate between the bounding assumptions, we conclude that the till was deposited 1 to 1.2 Ma. To summarize, it is encouraging that the method yields consistent results for weakly developed, truncated paleosols, as these are common in glacial sediment sequences in Minnesota and South Dakota, where well-developed paleosols are less frequent than they are in Nebraska and Iowa. However, analytical uncertainty, uncertainty in subsurface production rates, and uncertainty in the age of the overburden all contribute to a large total uncertainty in our age estimate for this till, although the uncertainty in the age of the overburden could be reduced by making additional measurements on tills higher up in the section.

CONCLUSIONS

1. *Outwash and river sediment in glaciated areas.* Unlike modern river sediment in unglaciated areas, both modern and ancient river sands in glaciated areas are nearly all derived from the recycling of older glacial deposits exposed in river cut banks. This sediment moves rapidly into fluvial systems without being appreciably exposed to the cosmic ray flux, and, when buried by later glacier advances, retains ^{10}Be and ^{26}Al concentrations that are inconsistent with surface exposure. Thus, neither glacial outwash or river sediment from regions affected by continental glaciation are good candidates for ^{10}Be–^{26}Al burial dating. On the other hand, the ^{26}Al and ^{10}Be concentrations of river sand can likely be used to distinguish glacially- and nonglacially-derived sediment in many rivers. We expect that river sands in regions affected only by restricted alpine glaciation are more likely to have nuclide concentrations consistent with surface exposure (for example, Stock and others, 2004). However, early and middle Pleistocene glacial deposits are often preserved in alpine forelands; in these regions, as well as in any nonglacial sedimentary system where Pliocene through middle Pleistocene sediment contributes to the river sediment load, inherited ^{26}Al and ^{10}Be in riverborne quartz will very likely complicate efforts at burial dating.
2. *Paleosols.* ^{26}Al and ^{10}Be measurements on quartz in paleosols developed on tills and then buried by later glacier advances can be used to date the overlying units. This method is most successful for soils that developed over a long period of exposure and consequently have high nuclide concentrations: the higher the nuclide concentrations at the time of burial, the less important many of the methodological uncertainties become. In contrast to exposure dating techniques (Putkonen and Swanson, 2003), the accuracy of this technique is at present limited by analytical uncertainties in AMS measurement. These uncertainties provide an incentive for further analytical improvements. As paleosols buried by later ice sheet advances are common in the stratigraphic record around the Laurentide Ice Sheet (and others), this method is widely applicable to dating and correlating Plio-Pleistocene glacial sediments.
3. *Contributions to regional glacial chronology.* We report several age determinations of regional interest in this paper. First, limiting ages derived from analyses of pre-Wisconsinan outwash and river sands from boreholes in the Minnesota

River Valley indicate that the lower part of this section was deposited 1.5 to 0.5 Ma, which is older than previously believed. Second, similar limiting ages in boreholes from the Prairie Coteau region of Minnesota and South Dakota indicate that the age of the lower part of the till section here is greater than 1 Ma. Also, analyses of river sand underlying the lowest till in the Prairie Coteau section indicate that this lowest till was deposited 2 to 1.5 Ma, and analyses of a paleosol interbedded with tills in this section suggest at least one ice sheet advance 1 to 1.2 Ma. Thus, the sequence of tills beneath the Prairie Coteau may contain a nearly complete record of late Pliocene through middle Pleistocene advances of the Laurentide Ice Sheet.

ACKNOWLEDGMENTS

Balco was supported by a graduate fellowship from the Fannie and John Hertz Foundation, by an internship from DOSECC, and by the J. Hoover Mackin Award of the Geological Society of America. We thank the South Dakota Geological Survey, Kelli McCormick in particular, for providing core samples from their archives, as well as Joe Mason for giving us access to Nebraska Conservation and Survey Division core 3-B-99 and John Boellstorff's archived cores at the University of Nebraska. Derrick Johnson and Pat Jaybush assisted in the laboratory. NSF grant EAR-0207844 supported travel and analytical work. We also appreciate reviews by D. Granger and J. Shulmeister.

APPENDIX

MAXIMUM LIMITING AGES FROM ^{26}Al AND ^{10}Be MEASUREMENTS

Here we describe how ^{26}Al and ^{10}Be analyses of a sample at a particular depth can be used to infer maximum limiting ages for some portion of their overburden.

Equation (3) can be rearranged to yield:

$$t_b = -\frac{1}{\lambda_j} \log \left[\frac{\left(N_j - \frac{P_j(z)}{\lambda_j} \right)}{\left(N_{j,0} - \frac{P_j(z)}{\lambda_j} \right)} \right] \tag{12}$$

We measure the present nuclide concentrations in a sample N_j and seek to choose the parameters z and $N_{j,0}$ to maximize the burial time t_b. We can only evaluate this formula if N_j and $N_{j,0}$ are both greater than, or both less than, $P_j(z)/\lambda_j$, the steady-state value at depth z. This reflects the fact that the nuclide concentration must always approach, and cannot cross, the steady-state value. Here we consider only the case where both are greater than the steady-state value. Because t_b must be greater than zero, this assumption also requires that $N_{j,0} > N_j$, that is, the initial nuclide concentration must be higher than the final nuclide concentration. Thus, if we have a sample whose present depth is z^M and a unit of overburden whose top has present depth z^*, we can only use this approach to infer a maximum age for this unit of overburden if $P_j(z^M - z^*) > N_j\lambda_j$ for both nuclides j. It is important that we are not inferring a maximum age for a sample, but a maximum age for a portion of the overburden which lies above some critical depth z^{crit}, where $P_j(z^M - z^{crit}) = N_j\lambda_j$. Figure A1 shows this relationship. In order to maximize t_b, we note that:

$$\frac{\partial t_b}{\partial P_j(z)} = \frac{1}{\lambda_j^2} \left[\frac{1}{N_j - \frac{P_j(z)}{\lambda_j}} - \frac{1}{N_{j,0} - \frac{P_j(z)}{\lambda_j}} \right] \tag{13}$$

and

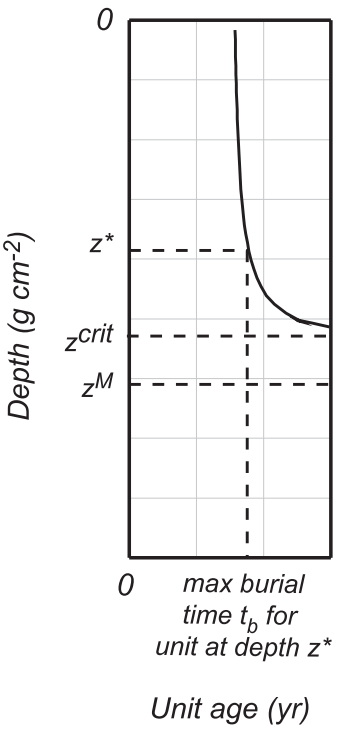

Fig. A1. Diagram showing the relationship between maximum possible age of portions of the overburden and their depth relative to a particular sample.

$$\frac{\partial t_b}{\partial N_{j,0}} = \frac{1}{\lambda_j\left(N_{j,0} - \dfrac{P(z)}{\lambda_j}\right)} \tag{14}$$

First, if $N_j > P_j(z)/\lambda_j$ and $N_{j,0} > N_j$ (as we have assumed above), $\partial t_b/\partial N_{j,0} > 0$ always. As expected, to maximize the burial time t_b we should choose the maximum possible initial nuclide concentration $N_{j,0}$.

Second, $N_j > P_j(z)/\lambda_j$ and $N_{j,0} > N_j$ also imply that $\partial t_b/\partial P_j(z) > 0$ always. This relationship means that to maximize t_b we should choose the maximum possible $P(z)$, that is, the minimum depth that the sample could have been buried at after deposition of the unit at depth z^*. This minimum depth is $z^M - z^*$. In effect, we are assuming that all of the overburden above the unit of interest was deposited instantaneously just before the present time, thus choosing the minimum possible burial depth for the sample since deposition of the unit of interest. The fact that the unit of overburden still exists shows that the sample could not have been less deeply buried since the deposition of that unit. Furthermore, we should also choose muon interaction cross-sections appropriately to yield the maximum $P_j(z)$.

We measure two nuclides j, so once we have chosen $z = z^M - z^*$, the choice of the $N_{j,0}$ is constrained by the relationship of the λ_j, that is, nuclide concentrations must have followed a burial trajectory defined by the production rates at the chosen burial depth, and the choice of nuclide concentrations that maximizes t_b is defined by the intersection of that burial trajectory with the simple exposure line. We obtain this

maximum age, $t_b^{\max}$, by solving the system of three equations consisting of equation (3) written for both ^{10}Be and ^{26}Al and equation (6).

Thus, each sample allows us to calculate a maximum limiting age for any unit of overburden whose top is above the critical depth z^{crit}. The unit whose top is at the critical depth z^{crit}, as the measured nuclide concentration is at steady state relative to that depth, could be infinitely old. The age of units higher up in the section is more closely limited, and the maximum age for units high up in the section asymptotically approaches the burial age for the sample calculated assuming initial nuclide concentrations on the simple exposure line and burial at infinite depth (fig. A1). If there are multiple samples in a single borehole, a maximum age calculated for a particular unit relative to a particular sample must also apply to all units above it according to the principle of superposition: thus, the maximum age limits for complete boreholes in figure 8 reflect the combination of several maximum age-depth curves such as those shown in figure A1. We have not taken analytical error into account in generating the maximum age limits in figure 8.

References

Balco, G., ms, 2004a, Measuring the density of rock, sand, and till: UW Cosmogenic Nuclide Lab Methods and Procedures. URL: http://depts.washington.edu/cosmolab/chem.html.

——— ms, 2004b, The sedimentary record of subglacial erosion beneath the Laurentide Ice Sheet: Ph.D. thesis, University of Washington, 136 p.

Balco, G., Stone, J.O.H., and Mason, J., 2005, Numerical ages for Plio-Pleistocene glacial sediment sequences by ^{26}Al/^{10}Be dating of quartz in buried paleosols: Earth and Planetary Science Letters.

Bettis, E. A., III, 1990, Holocene alluvial stratigraphy and selected aspects of the Quaternary history of western Iowa: Iowa City, Iowa, Midwest Friends of the Pleistocene, 37th Field Conference Guidebook, p. 197.

Bierman, P. R., Marsella, K. A., Patterson, C. J., Davis, P. T., and Caffee, M., 1999, Mid-Pleistocene cosmogenic minimum-age limits for pre-Wisconsinan glacial surfaces in southwestern Minnesota and southern Baffin Island: a multiple nuclide approach: Geomorphology, v. 27, p. 25–39.

Boellstorff, J., 1978a, Chronology of some late Cenozoic deposits from the central United States and the ice ages: Transactions of the Nebraska Academy of Sciences, v. 6, p. 35–48.

——— 1978b, A need for redefinition of North American Pleistocene stages: Transactions of the Gulf Coast Association of Geological Societies, v. 28, p. 65–74.

——— 1978c, North American Pleistocene stages reconsidered in light of probable Pliocene-Pleistocene continental glaciation: Science, v. 202, p. 305.

Cande, S. C., and Kent, D. V., 1995, Revised calibration of the geomagnetic polarity timescale for the Late Cretaceous and Cenozoic: Journal of Geophysical Research, v. 100, p. 6093–6095.

Clapp, E. M., Bierman, P. R., Schick, A. P., Lekach, J., Enzel, Y., and Caffee, M., 2000, Sediment yield exceeds sediment production in arid region drainage basins: Geology, v. 28, p. 995–998.

Ditchburn, R. G., and Whitehead, N. E., 1994, The separation of ^{10}Be from silicates: Third workshop of the South Pacific Environmental Radioactivity Association, p. 4–7.

Emiliani, C., 1955, Pleistocene temperatures: Journal of Geology, v. 63, p. 538–578.

Flint, R. F., 1955, Pleistocene geology of eastern South Dakota: U.S. Geological Survey Professional Paper 262, 173 p.

Forman, S. L., and Pierson, J., 2002, Late Pleistocene luminescence chronology of loess deposition in the Missouri and Mississippi River valleys, United States: Palaeogeography, Palaeoclimatology, Palaeoecology, v. 186, p. 25–46.

Forman, S. L., Bettis, E. A., III, Kemmis, T. J., and Miller, B. B., 1992, Chronologic evidence for multiple periods of loess deposition during the late Pleistocene in the Missouri and Mississippi River Valley, United States: implications for the activity of the Laurentide Ice Sheet: Palaeogeography, Palaeoclimatology, Palaeoecology, v. 93, p. 71–83.

Gansecki, C. A., Mahood, G. A., and McWilliams, M., 1998, New ages for the climactic eruptions at Yellowstone; single-crystal ^{40}Ar/^{39}Ar dating identifies contamination: Geology, v. 26, p. 343–346.

Gilbertson, J. P., and Lehr, J. D., 1989, Quaternary stratigraphy of northeastern South Dakota, *in* Gilbertson, J. P., editor, Guidebook for the Friends of the Pleistocene Field Conference, 3: United States, Friends of the Pleistocene Field Conference, p. 1-13.

Gosse, J. C., and Phillips, F. M., 2001, Terrestrial in situ cosmogenic nuclides: theory and application: Quaternary Science Reviews, v. 20, p. 1475–1560.

Granger, D. E., and Muzikar, P. F., 2001, Dating sediment burial with in situ-produced cosmogenic nuclides: theory, techniques, and limitations: Earth and Planetary Science Letters, v. 188, p. 269–281.

Granger, D. E., and Smith, A. L., 2000, Dating buried sediments using radioactive decay and muogenic production of ^{26}Al and ^{10}Be. Nuclear Instruments and Methods in Physics Research, B: Beam Interactions with Materials, v. 172, p. 822–826.

Granger, D. E., Kirchner, J. W., and Finkel, R. C., 1996, Spatially averaged long-term erosion rates measured from in situ-produced cosmogenic nuclides in alluvial sediment: Journal of Geology, v. 104, p. 249–257.

——— 1997, Quaternary downcutting rate of the New River, Virginia, measured from differential decay of cosmogenic ^{26}Al and ^{10}Be in cave-deposited alluvium: Geology, v. 25, p. 107–110.

Granger, D. E., Fabel, D., and Palmer, A. N., 2001, Pliocene-Pleistocene incision of the Green River, Kentucky, determined from radioactive decay of cosmogenic 26)Al and 10)Be in Mammoth Cave sediments: Geological Society of America Bulletin, v. 113, p. 825–836.

Hallberg, G. R., 1986, Pre-Wisconsinan glacial stratigraphy of the central Plains region in Iowa, Nebraska, Kansas, and Missouri, *in* Sibrava, V., Bowen, D. Q., and Richmond, G. M., editors, Quaternary Glaciations of the Northern Hemisphere: Oxford, Pergamon Press, Quaternary Science Reviews, v. 5, p. 11–15.

Hallberg, G. R., and Kemmis, T. J., 1986, Stratigraphy and correlation of the glacial deposits of the Des Moines and James lobes and adjacent areas in North Dakota, South Dakota, Minnesota, and Iowa, *in* Sibrava, V., Bowen, D. Q., and Richmond, G. M., editors, Quaternary Glaciations of the Northern Hemisphere: Oxford, Pergamon Press, Quaternary Science Reviews, v. 5, p. 65–68.

Hambrey, M. J., Barrett, P. J., and Powell, R. D., 2002, Late Oligocene and early Miocene glacimarine sedimentation in the SW Ross Sea, Antarctica; the record from offshore drilling, *in* Dowdeswell, J. A., and O'Cofaigh, C., editors, Glacier-influenced sedimentation in high-latitude continental margins: London, Special Publication Geological Society, n. 203, p. 105-128.

Heisinger, B., Lal, D., Jull, A. J. T., Kubik, P., Ivy-Ochs, S., Knie, K., and Nolte, E., 2002a, Production of selected cosmogenic radionuclides by muons: 2. Capture of negative muons: Earth and Planetary Science Letters, v. 200, p. 357–369.

Heisinger, B., Lal, D., Jull, A. J. T., Kubik, P., Ivy-Ochs, S., Neumaier, S., Knie, K., Lazarev, V., and Nolte, E., 2002b, Production of selected cosmogenic radionuclides by muons: 1. Fast muons: Earth and Planetary Science Letters, v. 200, p. 345–355.

Klein, J., Middleton, R., Giegengack, R., and Sharma, P., 1988, Revealing histories of exposures using in situ produced ^{26}Al and ^{10}Be in Libyan desert glass: Radiocarbon, v. 28, p. 547–555.

Lal, D., 1988, In situ produced cosmogenic isotopes in terrestrial rocks: Annual Reviews of Earth and Planetary Science, v. 16, p. 355–388.

——— 1991, Cosmic ray labeling of erosion surfaces: in situ nuclide production rates and erosion models: Earth and Planetary Science Letters, v. 104, p. 424–439.

Lal, D., and Peters, B., 1967, Cosmic ray produced radioactivity on the earth, *in* Sitte, K., editor, Handbuch der Physik: Berlin, Springer, p. 551–612.

Lineburg, J. M., ms, 1993, Sedimentology and stratigraphy of pre-Wisconsin drifts, Coteau des Prairies, eastern South Dakota: M.S. thesis, University of Minnesota.

Mangerud, J., Jansen, E., and Landvik, J. Y., 1996, Late Cenozoic History of the Scandinavian and Barents Sea ice sheets: Global and Planetary Change, v. 12, p. 11–26.

Mason, J. A., 2001, Surficial geology of the Fort Calhoun and Kennard quadrangles, Nebraska: Nebraska Conservation and Survey Division Open-File Report 56.

Nishiizumi, K., Winterer, E. L., Kohl, C. P., Klein, J., Middleton, R., Lal, D., and Arnold, J. R., 1989, Cosmic ray production rates of ^{26}Al and ^{10}Be in quartz from glacially polished rocks: Journal of Geophysical Research, v. 94, p. 17,907–17,915.

Partridge, T. C., Granger, D. E., Caffee, M., and Clarke, R. J., 2003, Lower Pliocene hominid remains from Sterkfontein: Science, v. 300, p. 607–612.

Patterson, C. J., 1997, Surficial geology of southwestern Minnesota, *in* Patterson, C. J., editor, Contributions to the Quaternary Geology of Southwestern Minnesota: Minnesota Geological Survey Report of Investigations No. 47.

——— 1999, Quaternary Geology - Upper Minnesota River basin, Minnesota: Minnesota Geological Survey Regional Hydrologic Assessment RHA-4.

Putkonen, J., and Swanson, T., 2003, Accuracy of cosmogenic ages for moraines: Quaternary Research, v. 59, p. 255–261.

Roy, M., Clark, P. U., Barendregt, R. W., Glasmann, J. R., and Enkin, R. J., 2004, Glacial stratigraphy and paleomagnetism of late Cenozoic deposits of the north-central United States: Geological Society of America Bulletin, v. 116, p. 30–41.

Setterholm, D. R., 1995, Quaternary Geology – Southwestern Minnesota: Minnesota Geological Survey Regional Hydrologic Assessment Series RHA-2.

Shackleton, N. J., Backman, J., Zimmerman, H., Kent, D. V., Hall, M. A., Roberts, D. G., Schnitker, D., Baldauf, J. G., Desprairies, A., Homrighausen, R., Huddlestun, P., Keene, J. B., Kaltenback, A. J., Krumsiek, K. A. O., Morton, A. C., Murray, J. W., and Westberg-Smith, J., 1984, Oxygen isotope calibration of the onset of ice-rafting and history of glaciation in the North Atlantic region: Nature, v. 307. p. 620–623.

Shackleton, N. J., 1995, New data on the evolution of Pliocene climate variability, *in* Vrba, E., Denton, G. H., Partridge, T. C., and Burckle, L. C., editors, Paleoclimate and Evolution, with emphasis on human origins: New Haven, Yale University Press, p. 242-248.

Shackleton, N.J., and Opdyke, N.D., 1973, Oxygen-isotope and paleomagnetic stratigraphy of equatorial Pacific core V28-238: oxygen isotope temperatures and ice volumes on a 10^5 year and 10^6 year scale: Quaternary Research, v. 3, p. 39–55.

Sheldrick, B. H., editor, 1984, Analytical Methods Manual 1984: Land Resource Research Institute, Research Branch, Agriculture Canada.

Soller, D. R., and Packard, P. H., 1998, Digital representation of a map showing the thickness and character of Quaternary sediments in the glaciated United States east of the Rocky Mountains: U.S. Geological Survey Digital Data Series DDS-38.

Stock, G., Anderson, R. S., and Finkel, R. C., 2004, Pace of landscape evolution in the Sierra Nevada, California, revealed by cosmogenic dating of cave sediments: Geology, v. 32, p. 193–196.

Stone, J.O.H., 2000, Air pressure and cosmogenic isotope production: Journal of Geophysical Research, v. 105, p. 23753–23759.

——— 2004, Extraction of Al and Be from quartz for isotopic analysis: UW Cosmogenic Nuclide Lab Methods and Procedures. URL: http://depts.washington.edu/cosmolab/chem.html.

Stone, J. O. H., Fifield, L. K., Beer, J., Vonmoos, M., Obrist, C., Grajcar, M., Kubik, P., Muscheler, R., Finkel, R., and Caffee, M., 2004, Co-precipitated silver-metal oxide aggregates for accelerator mass spectrometry of ^{10}Be and ^{26}Al: Nuclear Instruments and Methods in Physics Research B, v. 223-224, p. 272–277.

Wolkowinsky, A., and Granger, D., 2004, Early Pleistocene incision of the San Juan River, Utah, dated with ^{26}Al and ^{10}Be: Geology, v. 32, p. 749–752.